Applied Energy 298 (2021) 117200

Contents lists available at ScienceDirect

Applied Energy

journal homepage: www.elsevier.com/locate/apenergy

Sensitivity analysis on energy performance, thermal and visual discomfort of a prefabricated house in six climate zones in Australia

Sareh Naji [a], Lu Aye [a,*], Masa Noguchi [b]

[a] Renewable Energy and Energy Efficiency Group, Department of Infrastructure Engineering, Faculty of Engineering and Information Technology, The University of Melbourne, Vic 3010, Australia
[b] ZEMCH EXD Lab, Faculty of Architecture, Building and Planning, The University of Melbourne, Vic 3010, Australia

HIGHLIGHTS

- The energy use and indoor comfort of a prefabricated house was investigated.
- The TRNSYS model of the house was validated with a set of measured data.
- Using the validated model the sensitivities were analysed for six climate zones.
- Most sensitive envelope variables and trends against degree days were identified.
- Hierarchical cluster analysis created groups of cities with similar sensitivities.

GRAPHICAL ABSTRACT

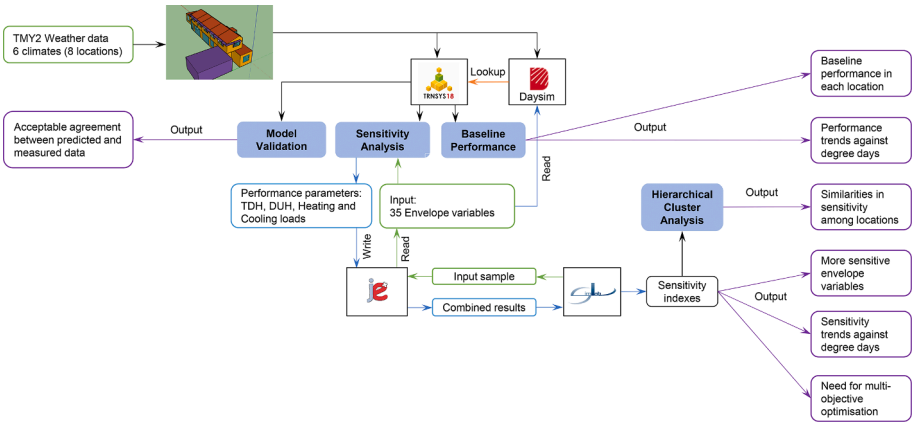

ARTICLE INFO

Keywords:
Sensitivity analysis
Building energy performance
Thermal comfort
Daylighting
Prefabricated building

ABSTRACT

In prefabricated buildings distinctive construction process and lightweight components affect design strategies and consequences. Therefore, to create more sustainable prefabricated buildings, it is important to understand the effects of their envelope parameters on energy performance and indoor environmental quality. Although previous research have investigated the effects of envelope on energy and indoor comfort outputs, the parameters of lightweight prefabricated envelope are not thoroughly considered. This article quantifies the effects of building envelope parameters on the energy use, thermal comfort and daylighting levels of a prefabricated house built in Australia. A building simulation model was developed and validated by comparing predicted with measured indoor temperatures of the house. The baseline performance for evaluation of energy consumption, thermal discomfort hours and daylight unsatisfied hours were carried out using Transient System Simulation (TRNSYS) tool. Series of regression-based sensitivity analyses (SAs) to identify the most sensitive parameters were conducted by coupling TRNSYS, jEPlus and SimLab. Applications in six climate zones were investigated. The important focus areas found by SA in each climate and their corresponding design responses can be applied across ranges of prefabricated building projects if built in similar climatic conditions. SA results revealed window

* Corresponding author.
E-mail address: lua@unimelb.edu.au (L. Aye).

https://doi.org/10.1016/j.apenergy.2021.117200
Received 28 November 2020; Received in revised form 2 May 2021; Accepted 26 May 2021

glazing and shading among the most influential parameters on all targeted performance outputs. The relationship between sensitivity levels to energy consumption and degree days indicated that the type of window has a higher impact on the reduction of energy use in the cooling dominated climates while insulation of wall was found a more effective strategy in heating-dominated climates.

Nomenclature

Symbols

DUH	daylight unsatisfied hours (h)
F	function
I_{space}	interior daylight illumination (lx)
I_{th}	the threshold levels daylight illumination (lx)
I_{th}	minimum threshold levels daylight illumination (lx)
m	sample size (-)
n	number of envelope parameters (-)
PMV	predicted mean vote (-)
T	total number of timesteps in a year (-)
TDH	thermal discomfort hours (h)
x	envelope parameter
y	input variable

Greek Symbols

Δt	simulation timestep (h)

Abbreviations

ACH	Air Changes per Hour (-)
BPS	Building Performance Simulation
CC	Correlation Coefficient (-)
CDD	Cooling Degree Day
DUH	Daylight Unsatisfied Hours (h)
GHG	Greenhouse Gas
HCA	Hierarchical Cluster Analysis
HDD	Heating Degree Day
IEQ	Indoor Environmental Quality
LHS	Latin Hypercube Sampling
MAE	Mean Absolute Error
MBE	Mean Bias Error
MOO	Multi-objective Optimisation
NCC	National Construction Code, Australia
PCC	Partial Correlation Coefficient (-)
PEAR	PEArson product moment coRrelation coefficient (-)
PRCC	Partial Rank Correlation Coefficient (-)
R^2	Coefficient of determination (-)
RMSE	Root Mean Square Error
SA	Sensitivity Analysis
SHGC	Solar Heat Gain Coefficient (-)
SPEA	SPEArman coefficient (-)
SRC	Standardised Regression Coefficient (-)
SRRC	Standardised Ranked Regression Coefficient (-)
TDH	Thermal Discomfort Hours (h)
TMY	Typical Meteorological Year
WMO	World Meteorological Organisation

1. Introduction

With the growing population and uncoordinated developments of the cities and challenges associated with increasing impacts of global warming, there is an essential need to enhance environmental and social sustainability of built environment [1]. As a response to environmental sustainability demands, more and more sectors throughout the world became eager to modify their processes to prioritise considerations for reduction of energy consumption. Buildings are responsible for a significant portion (nearly 40%) of the world's total energy consumption [2]. For instance, the primary energy consumption of residential and commercial buildings in the United States was about 11% of total primary consumption in 2019, while residential buildings were responsible for 6.5% [3]. In Australia, residential and commercial sectors are responsible for 7.4% and 5.4% of total energy consumption respectively [4]. Globally 60% of the total construction industry's energy consumption are associated with the residential sector [2]. Given the magnitude of this impact, it is important to explore strategies to reduce the energy consumption during entire lifecycle (creation, operation and end of life stages) of the built assets. Up to 70% of buildings' energy consumption is associated with the operational phase [5]. With increased understanding of the importance of achieving high quality and energy-efficient buildings, new standards and regulations, as well as design practices, are in place focusing on those aspects.

The social aspect of sustainable buildings attends to occupant's health and productivity within the indoor environments. Although the indoor environmental quality (IEQ) in houses need not necessarily be identical, there are common criteria that determine the levels of comfort in residential buildings. The ideal IEQ is the one that satisfies the occupants' comfort levels and does not increase the risk or severity of discomfort or illness [6]. IEQ can affect occupants' physical and mental health, and productivity. Various aspects of IEQ such as temperature, relative humidity, sound pressure level, lighting and view affect the occupants' quality of life to a great extent [6,7]. According to Haverinen-Shaughnessy et al. [8], indoor temperature and ventilation, as well as hygiene, affect the occupants' health and performance. Furthermore, the lack of sufficient daylight levels in dwellings causes important psychological problems [9]. Many studies have proved that the presence of adequate natural light increases productivity and helps to decrease stress [10]. Although no relationship of direct proportionality was found between energy consumption and thermal and visual comfort, the choice of architectuaral and construction solutions can affect both energy performance and IEQ levels in buildings [11].

With the growing demand for more sustainable, affordable and liveable built environments, prefabrication can serve as a more efficient way for designing, constructing and operating buildings compared to conventional construction methods. From a sustainability perspective, prefabrication has many potential benefits including reduced construction-induced carbon emissions [12], reduced construction waste and increased material quality. Currently prefabricated buildings market comprises 3% of total Australian construction industry with main focus on residential building sector [13,14]. Due to the standardisation of components, materials and quality control, prefabricated buildings are expected to have better overall quality [14]. This improved quality of prefabricated buildings leads to better insulation and airtightness affecting buildings' IEQ and energy efficiency performance [15]. Furthermore, lightweight construction of prefabricated buildings results in less thermal mass and more temperature variations affecting their thermal performance [16].

Some researchers attempted to evaluate the effects of prefabricated components on energy performance and IEQ of residential buildings. Ozarisoy and Elsharkawy [17] found summertime overheating issues in a residential building constructed with lightweight systems. It is also reported that new generation prefabricated lightweight buildings tend to use more energy for space conditioning [16]. Sonnick et al. [18]

identified low thermal mass as a potential issue with lightweight prefabricated buildings affecting their thermal efficiency. High level of indoor air humidity and condensation leading to mould growth were reported in prefabricated residential buildings [19]. Also, dissatisfaction with thermal conditions [20] and unacceptable noise levels [21] was reported in prefabricated schools. On the other hand, Petrosova and Petrosov [22] who evaluated the energy efficiency of a house with lightweight prefabricated wall construction systems in Leningrad, found that a high level of energy efficiency is achievable by using the lightweight components. Boafo et al. [15] highlighted that both conventional methods and prefabricated construction if using certain standards, can achieve high quality and desired performance.

Envelope parameters affect buildings' operational performance [12]. The choice of envelope parameters such as window size and orientation, glazing type, thermal mass, insulation, shading and air sealing can significantly affect the indoor thermal comfort, visual comfort as well as building's energy efficiency [14]. Ozarisoy and Altan [23] outlined that effective envelope retrofit strategies can result in significant improvement in building's energy performance. The Sensitivity Analysis (SA) conducted by Yıldız and Arsan [24] showed that the building annual heating and cooling loads are mostly affected by window size, window U-value, solar heat gain coefficient (SHGC) in hot-humid climates. In a similar study by Chen et al. [25] the sensitivity coefficient of the window SHGC in respect to cooling load was the highest of all selected factors. The type of glazing i.e. single, double, triple, and the size of the window directly affect the thermal and visual comfort as well as energy consumption of the buildings [24]. In an investigation by Wang et al. [26], the effects of occupant behaviour were found to be significant, especially in regard to window and solar shading system operations. Chen and Yang [27] found that the most influential factors on the energy performance of a passive high-rise residential building in climate zones of China are window U-value and window SHGC as well as the window to ground ratio. Window to wall ration was found to be the most sensitive parameter affecting thermal comfort in a design of informal settlement in Dharavi, Mumbai [28]. Gagnonet al. [29] identified window to wall ration, glazing SHGC and thermal conductivity of insulation material as the sensitive passive envelope materials affecting the energy performance of an office building in Quebec. In the same study, infiltration rate, temperature setpoints, and thickness and thermal conductivity of the insulation material were found sensitive to thermal comfort output.

Although previous researchers have investigated the effects of envelope parameters on energy performance and IEQ of buildings, there remains a lack of systematic guidelines and decision support in early design stages toward implementation of more sustainable building solutions [30]. Further, despite the existing literature on the performance of envelope components, there is still a lack of sufficient data on the impact of prefabricated components on IEQ and energy efficiency outputs. Understanding the effects of prefabricated envelope parameters can lead to more informed decisions in early design stages. Another important research gap identified is the lack of sufficient data on performance of a fixed prefabricated building design in various climatic conditions. A specific standardised prefabricated design can be implemented in various sites. Since the design parameters of the building should be adjusted based on climate conditions, it is important to understand their effects on design variables to incorporate in design guidelines [31].

This article aims to quantify the impact of various building envelope parameters on the energy use, thermal comfort and daylighting of a prefabricated house built in Australia. The applications of this study have been broadened to cover eight locations representing various Australian climate conditions across a range of latitudes. To investigate the applications of a specific prefabricated design on various climates, only the envelope parameters are selected as variables while other parameters such as size, shape and orientations are considered fixed. The assumptions made in the study are according to the general construction practices of prefabricated buildings. Therefore, the results and conclusions are specific to prefabricated buildings, while some specific findings can be generalised or applied in other lightweight buildings.

Building performance simulation (BPS) is a common method to evaluate the performance of buildings against certain targeted criteria. In the performance simulation of buildings some input parameters might have a greater effect on particular parameters. Therefore, it is important to investigate the influential building design parameters to maximise their performance. SA is a method to identify the relative importance of input parameters. It is defined as "The study of how the variations in the output of a model (numerical or otherwise) can be appointed, qualitatively, or quantitatively, to different sources of variation" [32]. The purpose of SA is to determine the links between variations in the independent input parameters and the ones in the independent output variables. The sensitivity coefficients obtained by SA can enhance the understanding of the model performance and its response to input variations useful for identification of possible changes to improve building performance [25]. It can also identify more and less significant parameters in the model which can lead to customisation of input variables [33] and constraints [34] in optimisation problems.

SA methods can be classified into two main categories: local and global. Local SA focuses on the impact of uncertain input parameters around a base case which is used as a reference point. By contrast, the ranges of input parameters for global SA cover the whole input space within the project-specific constraints [34]. Global SA can be implemented using various methods including regression-based, screening-based, variance-based or *meta*-model-based [34]. Some of the regression-based techniques used widely in the building simulation field are Pearson product moment correlation coefficient (PEAR), Partial Correlation Coefficient (PCC) and Standardised Regression Coefficient (SRC) and their corresponding rank transformation Spearman coefficient (SPEA), Partial Rank Correlation Coefficient (PRCC), and Standardised Ranked Regression Coefficient (SRRC) respectively [35]. By using SRC and SRRC, input and output parameters can be standardised as a result of subtracting the mean of the sample from original values and dividing the product by the standard deviation of the sample [20]. These coefficients are based on linear regression and have been used by several researchers in the field of building performance evaluation. Yildiz et al. [36] used SRRC to define the sensitive design parameters of low rise apartment buildings in hot-humid regions of Turkey. Chen et al. [25] used SRRC to evaluate the sensitivities of passive design parameters regarding the cooling and lighting energies of high-rise residential buildings in Hong Kong. Ignjatović et al. [37] implemented SA with SRRC to evaluate more influential design parameters of building design on energy consumption and occupant thermal comfort. Also, Li et al. [38] used SRRC and PRRC to measure the sensitivities of the design parameters in low energy buildings in Hong Kong.

In this article, baseline performance evaluation followed by a series of regression-based SAs were carried out on a validated building model of the house. The building model generated by TRNSYS was validated by comparing the measured and simulated indoor temperatures of the selected prefabricated house. The target output parameters were thermal discomfort hours (TDH), daylight unsatisfied hours (DUH) and annual heating and cooling loads. Input parameters were envelope characteristics which were selected based on the available components used in the construction of prefabricated buildings. A Hierarchical Cluster Analysis (HCA) was conducted to investigate patterns of similarities in responses among selected locations. This article presents the first section of a broader framework developed for conducting multi-objective optimisation in early design stages through a number of sequential rational steps. The steps include model development, model validation, sensitivity analysis (covered in this article), development of component's library presented in [39] and multi-objective optimisation (MOO) presented in [40]. SA prior to optimisation is an effective strategy to reduce the number of input parameters by identifying the most influential ones, those that should be optimised for achieving preferred outcomes [41]. The findings of this article are used in the definition of input parameters in [40] which conducts MOOs to minimise TDH, DUH

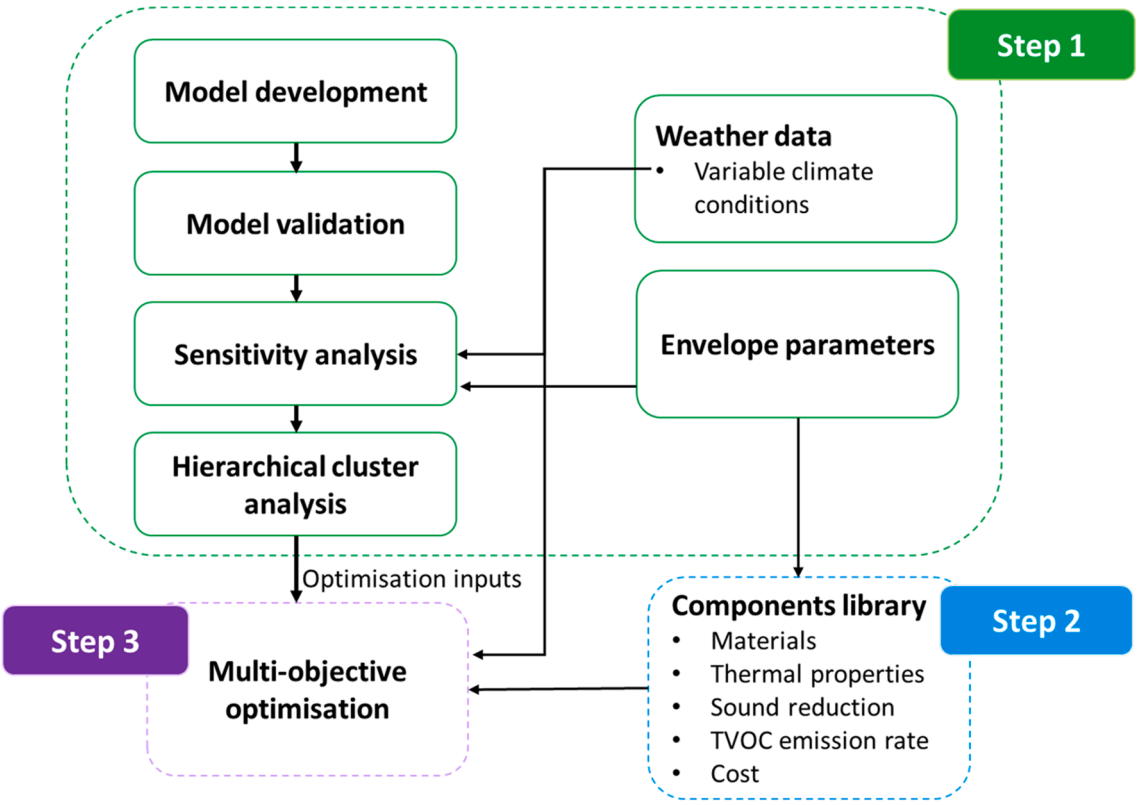

Fig. 1. Broader framework of the study [42]: Step 1 (this article), Step 2 [39], and Step 3 [40].

and life cycle costs of the selected building in six climates zones. MOO is an effective method used in early design stages to target multiple performance parameters that affect social, economic and environmental sustainability.

The novelty and scientific significance of this article is firstly the framework used which constructs an example to the researchers and practitioners in the field of BPS. The methods used for calibration and validation of the models as well as SA can be implemented by design practitioners in a diverse range of building projects. Implementing the proposed framework results in a more systematic approach leading to robust decision support in early design stages. On the other hand, baseline performance evaluation and SA conducted, contribute to the knowledge on the performance of lightweight prefabricated envelope components and their sensitivities. Another significance of this study is the methods and results of validation of a TRNSYS building model for the lightweight prefabricated building. The method used for calibration and validation of the model constructs an example for the similar practices in future. The selection of various climatic conditions provides more in-depth understanding of the impact of climate on the design decision-making while provides a comparison of building's performance and the important climate-specific focus areas. Furthermore, showcasing how a specific prefabricated design can be optimised for each climatic condition, would help understand the potential applicability of standardised design approach for prefabrication to inform future research and applications.

2. Methods

This article presents the first section of a broader framework developed for conducting MOO in early design stages through a number of sequential rational steps [42]. The steps include model development, model validation, SA (covered in this article), development of component's library presented in [39] and MOO presented in [40]. Fig. 1 presents the steps included in the broader framework of this study. In the following sections, the details of simulations, baseline performance evaluation, SA and HCA conducted are presented.

2.1. Simulation

This subsection provides detailed information on the baseline building, model assumptions, selected locations and tools used for the simulations and SA.

2.1.1. Selected locations and weather data

Understanding the geospatial distribution of climatic conditions is an essential step for building design which meets comfort requirements and achieves good energy efficiency [23]. In this investigation, six climate zones in Australia: Oceanic (Melbourne and Hobart), Humid Subtropical (Brisbane and Sydney), Hot Summer Mediterranean (Perth), Cold Semi-arid (Mildura), Hot Desert (Alice Springs) and Savanna (Darwin), were selected to represent a wide range of latitudes and climate classifications. Fig. 2 shows the selected locations with their climate classifications based on the Köppen-Geiger climate map of Australia [43]. Appendix Table A1 shows the populations, latitudes, longitudes as well as the Australian climate zones (as defined by the National Construction Code (NCC)) of the selected locations. NCC is the Australian building code which prescribes minimum requirements on various aspects of building design including safety and amenity, structural design, energy efficiency and liveability [44]. Table 1 shows the begin and end dates of the heating and cooling seasons of the selected climates. It should be noted that these dates were derived from the corresponding hourly ambient air temperatures in the Typical Meteorological Year (TMY) data files.

The heating and cooling seasons for each location were determined by obtaining the daily average indoor temperature of the selected building. These temperatures were identified by running simulations in different locations on free-running mode i.e. no heating and cooling. The heating season is the period when the average daily temperature falls

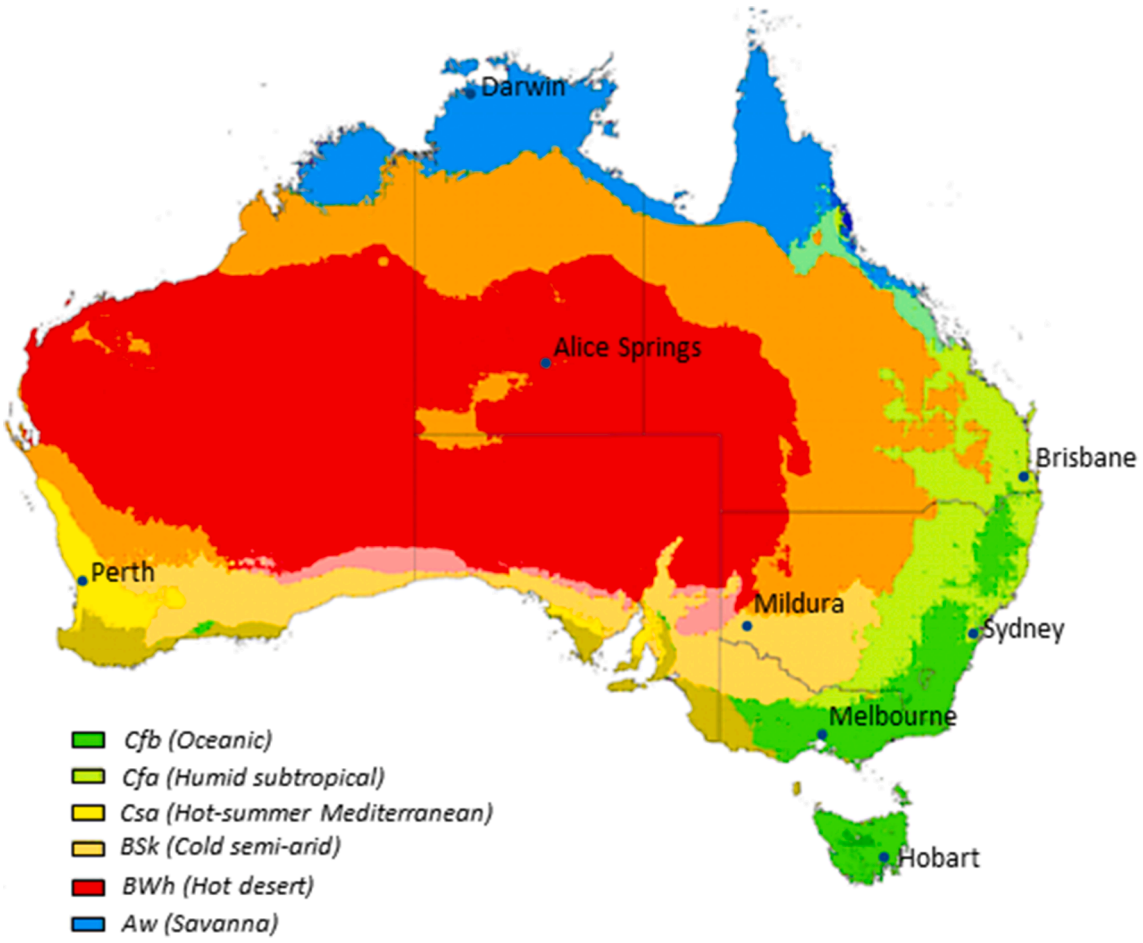

Fig. 2. The selected locations shown on Köppen-Geiger climate map of Australia [43].

Table 1
The features of selected locations.

Location	Climate Code[1]	Latitude (° S)	Heating season				Cooling season			
			HDD[2]	Begin	End	Days	CDD[3]	Begin	End	Days
Darwin	*Aw*	12.4634	1	–	–	0	2205	01/01	31/12	365
Alice Springs	*BWh*	23.6980	687	01/06	10/08	71	1087	01/10	15/04	196
Brisbane	*Cfa*(B)	27.4698	463	10/06	15/07	36	353	20/10	01/05	193
Perth	*Csa*	31.9505	762	01/06	10/09	102	297	10/11	10/04	151
Sydney	*Cfa*(S)	33.8688	564	01/06	15/08	76	125	10/11	10/04	151
Mildura	*BSk*	34.2080	1136	10/05	20/09	134	476	10/11	10/04	151
Melbourne	*Cfb*(M)	37.8136	1439	20/05	15/09	119	115	10/11	20/04	161
Hobart	*Cfb*(H)	42.8821	2414	01/01	31/12	365	14	–	–	0

Indoor setpoint temperature for season definition is 18 °C for heating and 26 °C for cooling.
[1] Where two location have the same climate classification the initial letter of location name is included with the climate code.
[2] HDD reference temperature is 18 °C.
[3] CDD reference temperature is 24 °C [51].

below 18 °C while the cooling season is determined based on the dates when the daily average temperature was above 26 °C.

The weather data files for the selected locations were generated using Meteonorm software which uses data from the World Meteorological Organisation (WMO) [45]. Its database contains meteorological information from more than 8,000 weather stations which can be assembled into a weather file in formats and time intervals. The weather data file embed necessary information required for energy simulation including solar radiation, temperature, relative humidity, sky cover, wind direction and speed. In this investigation, the default settings: 'Time period for temperatures' and 'Time period for radiation' were selected in the software as recommended in the manual [46]. TMY2 data format was used and solar time was selected for the file generation. In order to foresee overall picture of climatic conditions and thermal comfort parameters, monthly average solar radiations received on the horizontal plane,monthly average ambient air temperatures, and psychometric chart for each case study location are provided in Figs. A1 and A2 in Appendix A. Software tools EnergyPlus's 'Weather Converter Program, Version 8.1.0' [47,48] and 'Climate Consultant 6.0' [49] were utilised to generate psychrometric charts.

2.1.2. Building model

An existing building (Fig. 3 and Fig. 4) was chosen from the current prefabricated projects in Australia. The building is a two-story five-

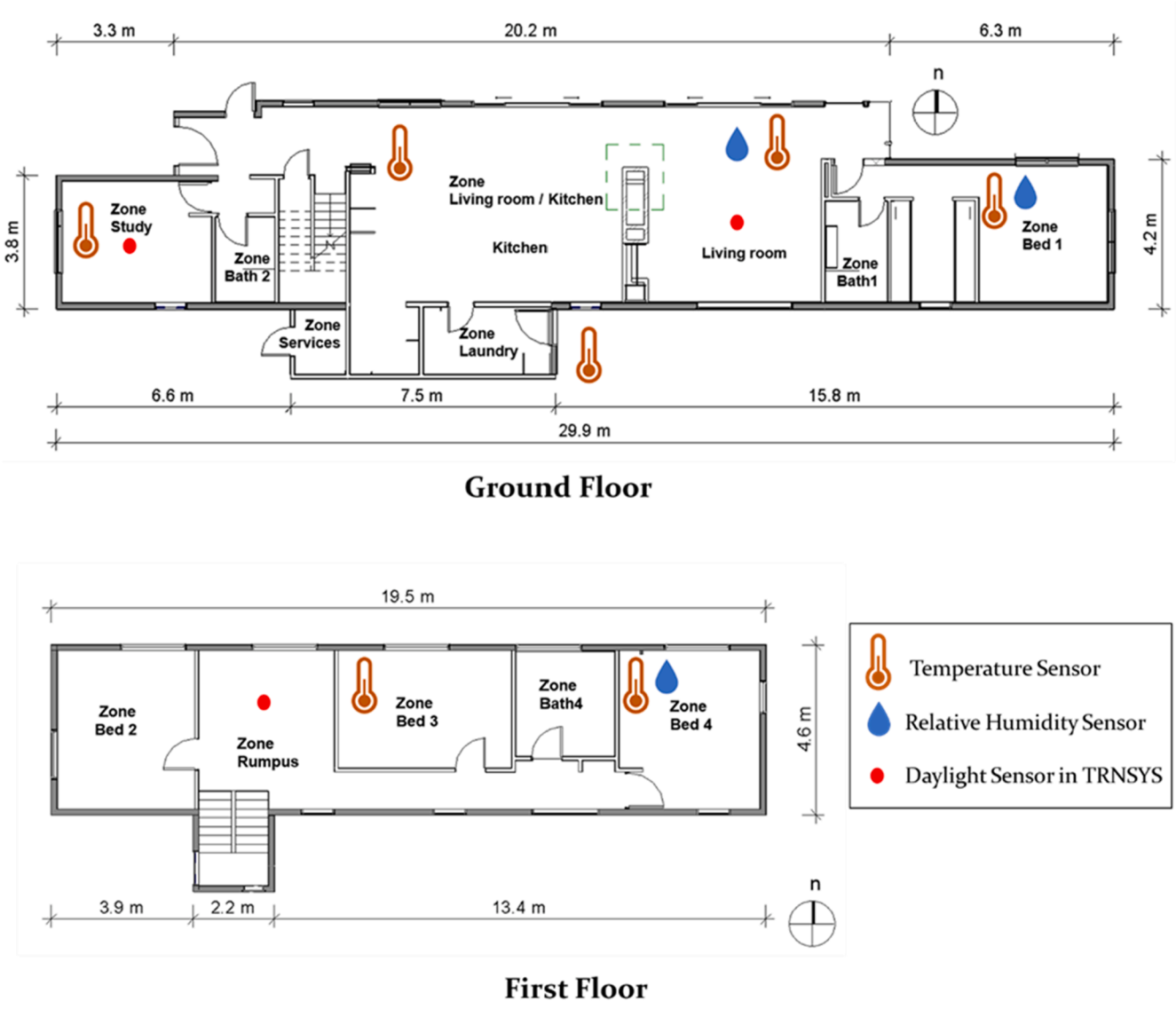

Fig. 3. The plan of the selected building and locations of data loggers and daylight sensors.

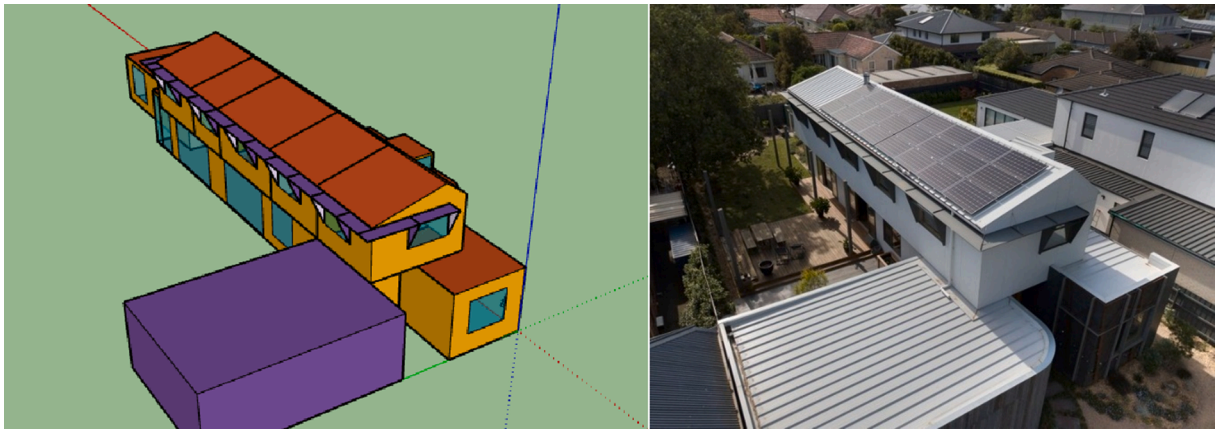

Fig. 4. Left: 3D SketchUp model; Right: View of the building [52].

bedroom house located in Melbourne. The ground floor area is 144.5 m^2, the first-floor area is 69.5 m^2 and ceiling height is 2.8 m. Bedrooms, Study room and Living room are conditioned while other spaces are in free-running mode. Materials used in the construction of this building are provided in Table A3 in Appendix A. Also, additional images of the selected building and its materials are provided in Fig. A3 in Appendix

Table 2
Ranges of input variables in SA of the selected building.

No.	Input variable	Unit	Range	Baseline value
V1	Exterior wall cladding thickness	m	0.005-0.100	0.009
V2	Exterior wall cladding specific heat	kJ $kg^{-1}K^{-1}$	0.4-1.1	0.88
V3	Exterior wall insulation thickness	m	0.05-0.25	0.15
V4	Exterior wall insulation conductivity	W $m^{-1}K^{-1}$	0.025-0.055	0.036
V5	Exterior wall interior finish thickness	m	0.005-0.100	0.012
V6	Exterior wall interior finish specific heat	kJ $kg^{-1}K^{-1}$	0.4-1.1	1.2
V7	Roof cladding thickness	m	0.001-0.100	0.001
V8	Roof cladding specific heat	kJ $kg^{-1}K^{-1}$	0.4-1.8	1.8
V9	Roof insulation thickness	m	0.05-0.45	0.15
V10	Roof insulation conductivity	kJ $h^{-1}m^{-1}K^{-1}$	0.025-0.055	0.036
V11	Roof Airspace resistance	m^2 K W^{-1}	0-0.23	0.17
V12	Floor concrete thickness	m	0.1-0.7	0.15
V13	Floor concrete specific heat	kJ kg^{-1} K^{-1}	0.4-1.1	1.0
V14	Floor insulation thickness	m	0.050-0.100	NA
V15	Floor insulation conductivity	W $m^{-1}K^{-1}$	0.025-0.055	NA
V16	North windows shading factor (GF)	-	0.0-0.6	0.0
V17	South windows shading factor (GF)	-	0.0-0.6	0.0
V18	East windows shading factor (GF)	-	0.0-0.6	0.0
V19	West windows shading factor (GF)	-	0.0-0.6	0.0
V20	North windows shading factor (FF)	-	0.0-0.6	0.0
V21	South windows shading factor (FF)	-	0.0-0.6	0.0
V22	East windows shading factor (FF)	-	0.0-0.6	0.0
V23	West windows shading factor (FF)	-	0.0-0.6	0.0
V24	North windows' type	-	No.101-14308[1]	No.201
V25	South windows' type	-	No.101-14308[1]	No.201
V26	East windows' type	-	No.101-14308[1]	No.201
V27	West windows' type	-	No.101-14308[1]	No.201
V28	North windows' area	m^2	0.8-5.0	2.59
V29	South windows' area	m^2	0.8-5.0	1.33
V30	East windows' area	m^2	0.8-5.0	2.38
V31	West windows' area	m^2	0.8-5.0	2.61
V32	North glazing visual transmittance	-	10-90	70
V33	South glazing visual transmittance	-	10-90	70
V34	East glazing visual transmittance	-	10-90	70
V35	West glazing visual transmittance	-	10-90	70

[1]The window ID as specified in window library

The window ID as specified in window library

A. The R-value of the roof section is 4.97 $m^2K.W^{-1}$ while the R-value of the wall section is 4.3 $m^2K.W^{-1}$. Those values are compliant with the insulation requirement of NCC [The minimum required R-value of the roof 4.6 $m^2K.W^{-1}$in Oceanic (Melbourne and Hobart) and 4.1 in other climates while the minimum required R-value for wall section is 2.8 $m^2K.W^{-1}$ in all climates]. The building also complies with the NCC ventilation requirements (the ventilation area not<5% of the space floor area for habitable rooms as well as bathrooms and laundry) [44]. The floor areas of the rooms, glazing areas and the glazing to floor area ratio are shown in Table A2 in Appendix A. In addition, ventilation air change rates for Bathroom1, Bathroom2, Bathroom3, kitchen and living area are set according to [50] 6 ACH, 5 ACH, 2.9 ACH, 0.4 ACH and 0.35 ACH respectively.

The building is a single-family house where parents and four children live. The schedules for occupants, light and appliances were defined according to assumed typical daily routines. The occupant schedules for spaces are shown in Fig. A4 in Appendix A. These schedules are derived from the internal load tables defined by the Nationwide House Energy Rating Scheme (NatHERS) [53]. The internal heat gain from people was assumed to be 130 W per person when present. Clothing level 0.5 Clo was used for summer while 1 Clo was used for winter [48]. The daylighting sensor points (circles in Fig. 3) were located in different zones to monitor the illuminance levels.

Table 3
Window types used as input parameters.

ID no.	Description	#Panes	Infill gas	Glass thickness and infill (mm)	U-value W $m^{-2}K^{-1}$	SHGC (-)	Frame U-value W $m^{-2}K^{-1}$
101	Single clear	1	–	5	5.72	0.84	2.27
106	Single clear	1	–	14	5.44	0.73	2.27
3416	Double clear	2	Ar90	6/16/6	2.82	0.64	2.27
200	Double low E (e2 = 0.04)	2	Air	4/12/4	1.69	0.66	2.27
201	Double low E (e2 = 0.037)	2	Kr90	6/16/6	1.10	0.62	2.27
202	Double low E (e1 = 0.013)	2	Ar90	6/16/4	1.01	0.33	2.27
3428	Double low E (e1 = 0.012)	2	Ar90	6/16/4	1.01	0.22	2.27
400	Double low E (e2 = 0.037)	2	Ar90	4/10/4	1.07	0.62	2.27
401	Double low E (e2 = 0.03)	2	Ar90	6/16/4	1.08	0.47	2.27
300	Triple low E (e1 = 0.037)	3	Ar90	4/12/4/12/4	0.76	0.49	2.27
301	Triple low E (e1 = 0.013)	3	Ar90	6/12/4/12/4	0.73	0.30	2.27
500	Triple low E (e1 = 0.01, e3 = 0.03)	3	Ar90	6/12/4/12/4	0.72	0.26	2.27
501	Triple low E (e1,e3 = 0.03)	3	Ar90	6/12/4/12/4	0.74	0.23	2.27
3500	Triple low E (e1, e3 = 0.092)	3	Kr90	4/12/4/12/4	0.65	0.62	2.27
3515	Triple low E (e1 = 0.012)	3	Ar90	6/14/4/14/4	0.64	0.20	2.27
14,300	Triple low E (e1,e3 = 0.037)	3	Ar90	4/16/4/16/4	0.61	0.50	2.27
14,308	Triple low E (e1,e3 = 0.037)	3	Kr90	4/12/4/12/4	0.52	0.50	2.27

2.2. Software tools

TRNSYS [54] and associated graphical user interfaces were used for building energy and lighting performance simulations. TRNSYS is a powerful simulation engine that handles the complex functions of the transient systems [55]. The user-friendly interface and modular structure of TRNSYS make it a flexible tool that can be used for different applications. TRNSYS has embedded functions to incorporate inputs and outputs of daylight simulations through coupling with DAYSIM. TRNSYS 3D graphical interface was applied to generate the 3D model of the building. This model was then transferred to TRNBuild interface to assign non-geometrical attributes in TRNSYS. TRNSYS Simulation Studio interface [54] was used to assemble other TRNSYS types. DAYSIM [56] (daylight simulation software capable of predicting daylight illuminance inside and outside the building) was used for daylight simulations. The software uses Radiance [57] as the simulation engine. It is accessible through TRNBuild interface and can read the building information to run daylight simulations. The results can be transferred to building model as lookup tables [55].

The parametric runs were carried out using jEPlus [58], a user-friendly tool that allows parametric runs by coupling with energy simulation tools such as TRNSYS, EnergyPlus and DOE-2. Due to the graphical interface, results' reliability and inter-operability with energy simulation and SA tools this software tool has been selected. SimLab [59] (a Monte Carlo based uncertainty and SA tool) was used for conducting SA, the creation of batch files for input parameters population and the post-processing of outputs.

2.3. Baseline performance evaluation

For the performance simulation of the selected building 15 thermal zones were assigned (Fig. 3). Each room was assigned as a zone and attic space was also assigned as a zone. The setpoints for heating (18 °C) [60] and cooling (26 °C) were selected for the conditioned zones. The operating schedule for heating was assumed to be 8:00 to 23:00. The heating was not active during night-time, to reflect the general night-time operation of residential heating in Australia. The cooling was assumed to be operating during 8:00 to 23:00 for the Living room and Rumpus room and during the night-time (23:00 to 8:00) for bedrooms. For the study locations with daylight saving, whether it is in operation or not, was considered in the TRNSYS model. The heating and cooling seasons as defined in Table 1 were applied in the building model. The building is assumed to be conditioned during heating and cooling seasons while it is on free-running mode during the remainder of the year. To be consistent with the weather data files and TRNSYS calculations all the schedules in the model applied local solar time. Also, the model settings were adjusted for the locations that observe daylight saving times. The baseline thermal performance of the selected building was simulated for each location. The building model was calibrated and validated by using sets of measured data on temperature and relative humidity as described in Appendix B.

2.4. Sensitivity analysis

A commonly used regression-based SA is a fast and simple method which generates more quantitative measures of sensitivity. In this method, a mapping from input parameters to output variables is carried out using a Monte Carlo experiments, Eq. (1) [35].

$$y_i = f(x_{1n}, x_{2n}, \ldots, x_{in}) \quad i = 1, \ldots, m \tag{1}$$

where n is the number of independent input parameters and m is the sample size.

Uniform distribution was selected to generate the sample since all the input parameters are equally probable for a new building [37]. Latin Hypercube Sampling (LHS) method was used to generate an input sample. The minimum population size recommended by SimLab is 10 times the number of input parameters (350 in this study) [35]. A larger population size was selected (1,000) for a more accurate investigation. This method tends to provide satisfactory results regardless of the sample size [61] and has been used by several researchers in similar SA studies. Chen et al. [25] used LHS sampling in for carrying out a SA of energy, daylight and airflow network in public housing projects in Hong Kong. In another study, Chen et al. [62] used the same sampling method to investigate the effects of passive design parameters on energy, daylighting and thermal comfort in high-rise residential projects. Also, Yildiz et al. [36] and Li et al. [38] used LHS for sampling in their SA studies.

2.4.1. Input parameters

The input parameters (Table 2) were selected from the influential envelope characteristics. Constraints were applied to their ranges according to the available prefabricated components as listed in prefabricated components' library [39] and the requirements of the NCC. The range of window area was based on the requirements of the NCC for minimum natural ventilation (as specified in Section 2.1.2.) as well as the practicality to fit within the building geometry. The influential envelope characteristics considered are the thermal mass of external walls and roof, the thermal resistance of insulation, glazing type and dimensions, and shadings. The ranges of window types and their characteristics are shown in Table 2. The types of windows are predefined in the TRNSYS built-in window library. Varieties of materials and windows were selected based on commonly available products in the market

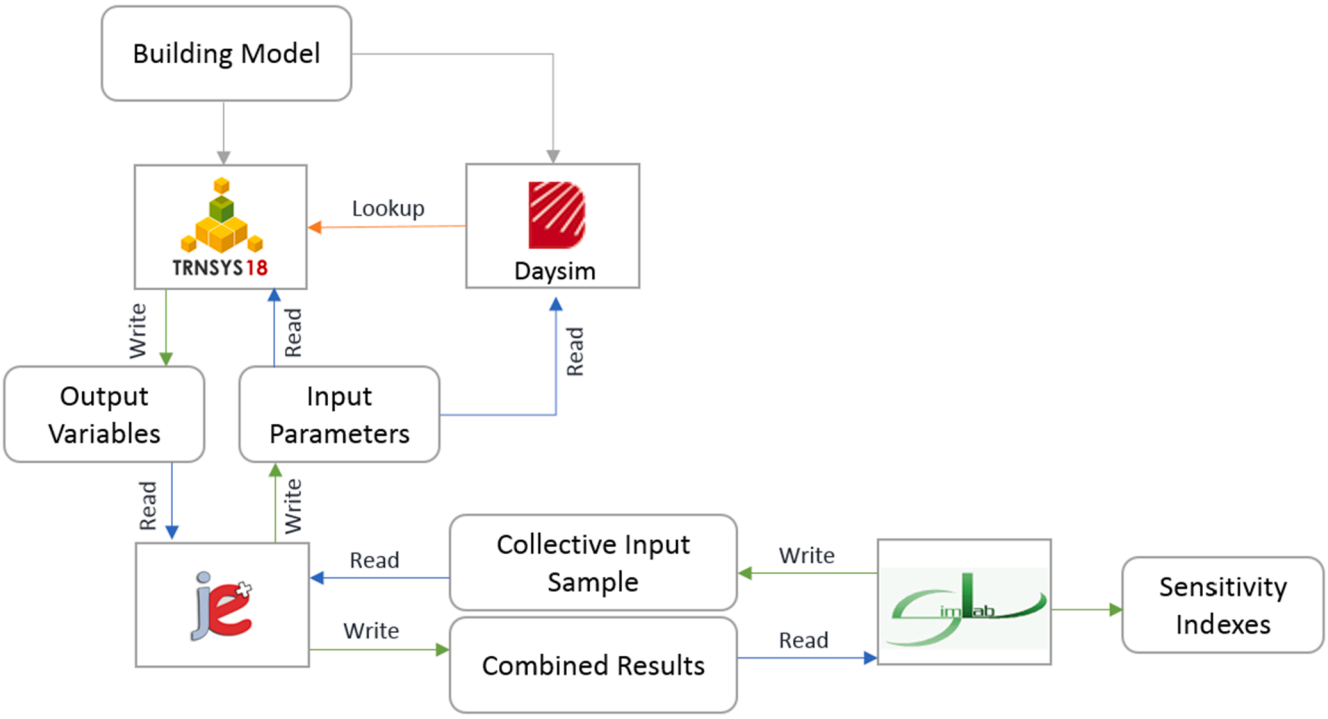

Fig. 5. SA workflow.

which are used in the construction of prefabricated buildings. In other words, the envelope characteristics were selected to represent light-weight components used in prefabricated buildings.

TRNSYS defines the shading factor as the fraction of the non-transparent area to the whole window area. For detailed investigations, the shading factor was considered separately on different floors and façade orientations. Also, the area and types of windows were considered as separate factors on various façade orientations (Table 3). The effect of shading on daylighting was simulated by applying shading factor in the Radiance material (glass) visual transmittance.

Since this study investigates the effects of envelope parameters on a specific prefabricated building design in various climates, the factors such as building size, shape, orientation and ventilation rates are considered fixed. The building orientation is fixed in a way that the living areas are equator facing to obtain sufficient natural daylight and solar heat. The assumed ventilation and infiltration rates are specified in Section 2.1.2.

2.4.2. Output variables

Annual heating and cooling loads, TDH and DUH were identified as the output parameters in the SA. TDH is calculated based on ASHRAE 55–2017 Predicted Mean Vote (PMV) based thermal comfort criteria [63]. PMV represents the votes of a large population on the thermal conditions of a space. It is expressed in a seven-point Likert scale (from −3 to 3) where −3 represents 'too cold' and 3 represents 'too warm'. Scale '0' represents the thermal neutrality (lowest dissatisfied votes amongst the population) [64]. TDH during occupied hours is calculated using Eq. (2). In compliance with ASHRAE 55–2017, the acceptable range of PMV was set as $-0.5 \leq PMV \leq 0.5$.

$$TDH = \sum_{t=1}^{T} \begin{cases} 0 \ \ for\ |PMV| \leqslant 0.5 \\ \Delta t\ for\ |PMV| > 0.5 \end{cases} \tag{2}$$

where T is the total number of timesteps in a year and Δt is the simulation timestep in hour unit.

A similar approach was used to obtain DUH during occupied hours (see Eq. (3)). A value of '0' was used if sufficient daylight existed and '1' where it did not. The duration of artificial lighting was not considered in this investigation. The threshold levels daylight illumination 300 lx and 400 lx were assigned for the Living room and Study room respectively [65].

$$DUH = \sum_{t=1}^{T} \begin{cases} 0 \ \ for\ I_{space} \geqslant I_{th} \\ \Delta t\ for\ I_{space} < I_{th} \end{cases} \tag{3}$$

where I_{space} is the interior daylight illumination and I_{th} is the threshold levels daylight illumination and Δt is the simulation timestep in hour unit.

2.4.3. SA workflow

Fig. 5 illustrates the workflow for the SA applied. For carrying out regression-based SA for this investigation, the input parameters and their ranges were defined using SimLab and the sample population of 1,000 was generated accordingly. The search strings of the same input parameters were added in jEPlus project while the same delimiters were placed in respected sections on the TRNSYS building input file. The batch sample file generated in SimLab was inputted in the jEPlus project after ensuring that the sample data file could be read correctly by jEPlus.

TRNSYS model reads daylight simulation output file during execution. Therefore, the daylight simulation results must be generated prior to TRNSYS simulation. To facilitate this sequential execution of simulations, jEPlus execution command was written to call this engine to run and complete DAYSIM execution prior to TRNSYS simulation. The SA runs were carried out using a 16-core virtual machine so that 16 parallel runs could be executed. After completing the simulations in jEplus the collective output results were modified to SimLab format and imported into SimLab. SRRC was selected as the sensitivity coefficient for this investigation. By importing the SimLab input and output files the SA was carried out and the SRRC values were obtained.

2.5. Hierarchical cluster analysis

Hierarchical Cluster Analysis (HCA) is a method to generate clusters of objects by measuring the distances between variables attributed to

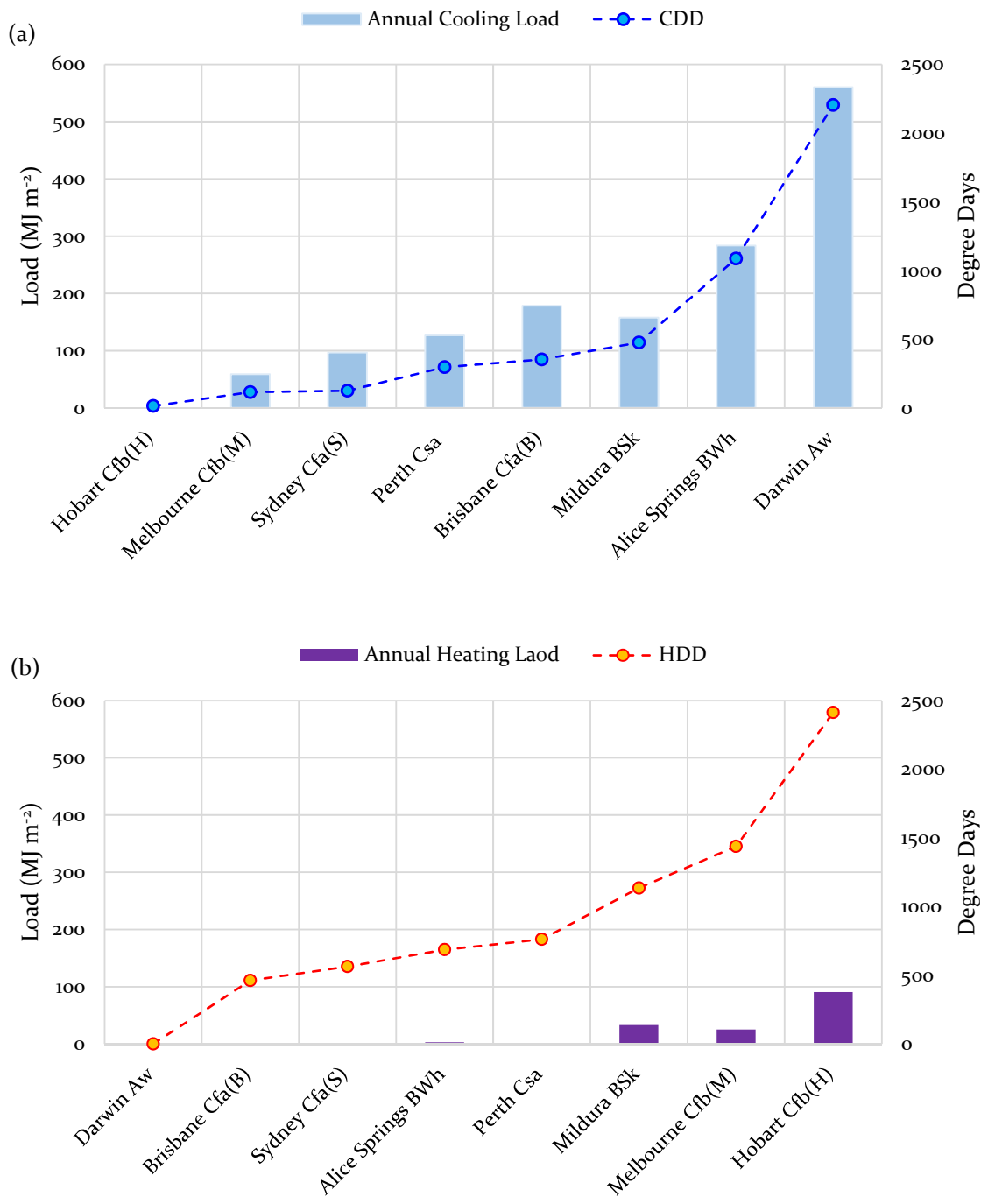

Fig. 6. Annual (a) cooling and (b) heating loads of the selected building in selected locations.

them. HCA groups the objects with the closest distance into a specified number of clusters. The HCA results can be presented using a dendrogram which is the visual representation of the clustered objects. In this study agglomerative HCA was employed to visualise the similarities of SA results among various locations. In this method, each location represents one cluster at the beginning of the analysis. The clusters would be generated by merging the locations with similar sensitivities regarding certain outputs i.e. heating load, TDH, etc. [66].

SPSS [67] was used for carrying out HCA. The Centroid Clustering method was selected in which the distance between cluster centroids (the average value of objects in the cluster on sets of variables representing the object) is used as the measure for the similarity between clusters. Squared Euclidean distance is used as the method for measuring distance in which the sum of squared distances is calculated and used as interval measures. This is recommended for measuring the Centroid clustering method [68]. The output is presented in the form of dendrograms which show the grouping of locations with different similarity levels. Depending on the number of expected clusters, the perception of the results of HCA can be different. By drawing a vertical line on the dendrogram and moving the line horizontally, various scenarios with different numbers of clusters can be explored.

3. Results

The results of baseline performance evaluation, SA and HCA are presented in this section.

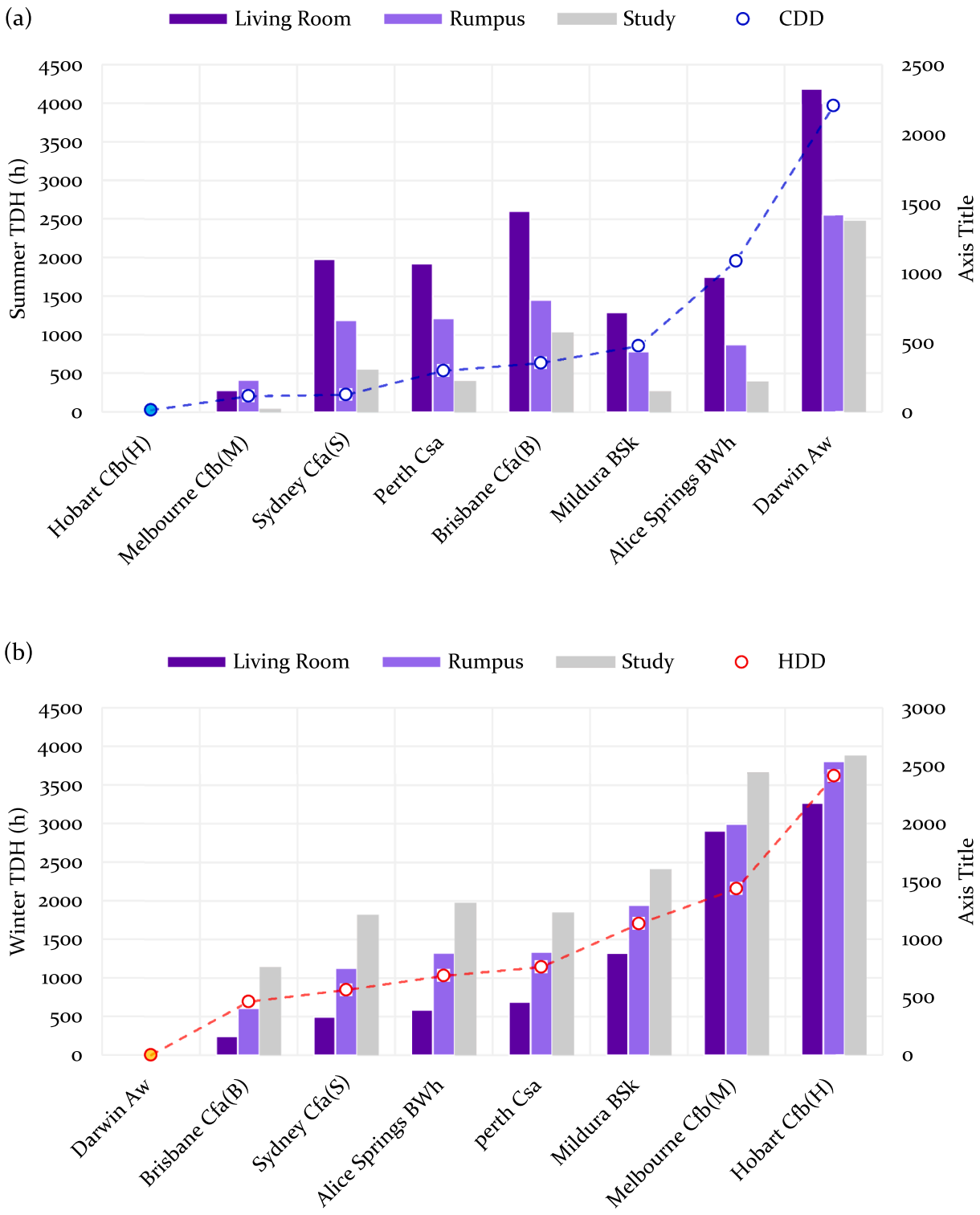

Fig. 7. Annual (a) summer and (b) winter thermal discomfort hours (TDH) of Living room, Study Room and Rumpus room mapped to heating and cooling degree days in selected climate zones.

3.1. Baseline performance

The energy performance, TDH and DUH in three zones of the building were evaluated. Fig. 6 shows the annual heating and cooling load per unit floor area. The results are provided for each climate zone with their respective heating degree day (HDD) and cooling degree day (CDD). In this investigation, indoor setpoint temperature is 18 °C for heating and 26 °C for cooling. This setpoint has been selected based on recommendations of [60] in order to save energy in residential buildings. The monthly values of cooling and heating loads are provided in Fig. C1 and Fig. C2 of Appendix C. Fig. 7 shows the summer and winter TDH values for three zones of the building: Living room, Rumpus room and Study room in all selected locations and their respective CDD and HDD. Fig. 8 shows the DUH values of the three zones of the selected building in selected locations. The monthly TDH and DUH values of the same building zones are provided in Appendix C.

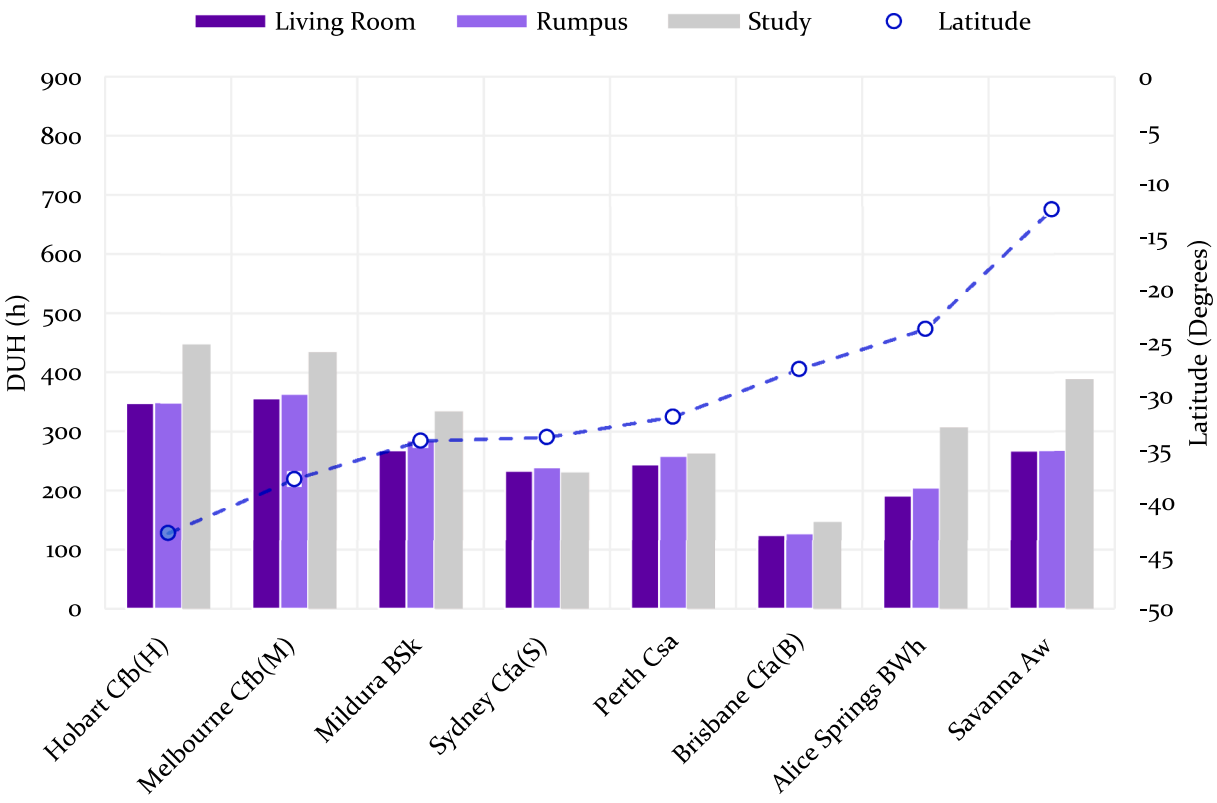

Fig. 8. Annual DUH of Living room, Study Room and Rumpus room mapped to latitude in all selected locations.

Table 4
SRRC of input parameter for the (a) heating and (b) cooling load.

	(a) Sensitivity to Heating Load							(b) Sensitivity to Cooling Load						
Input	*BWh*	*Cfa*(B)	*Csa*	*Cfa*(S)	*BSk*	*Cfb*(M)	*Cfb*(H)	*Aw*	*BWh*	*Cfa*(B)	*Csa*	*Cfa*(S)	*BSk*	*Cfb*(M)
V3	3	3	3	3	3	3	3	-	-	-	-	-	-	-
V4	5	5	5	5	5	5	5	-	-	-	-	-	-	-
V5	4	-	-	-	-	-	-	-	-	-	-	-	-	-
V9	4	4	4	4	4	4	4	-	-	-	-	-	-	-
V11	4	4	4	4	4	4	4	-	-	-	-	-	-	-
V16	7	7	7	6	7	7	7	3	3	3	3	3	3	3
V18	-	-	-	-	-	-	-	-	-	-	4	-	-	-
V20	5	5	5	5	5	5	5	-	-	-	-	-	-	-
V24	-	-	-	-	-	-	-	3	3	3	3	3	3	3
V25	4	4	4	4	4	4	4	-	-	-	-	-	-	-
V26	-	-	-	-	-	-	-	-	-	4	4	-	-	-
V27	-	-	-	-	-	-	-	-	-	4	-	-	-	-
V28	3	3	4	4	3	3	3	6	6	6	6	6	6	6
V29	-	-	-	-	-	-	-	6	5	6	6	6	6	6
V30	-	-	-	-	-	-	-	5	5	5	6	5	5	5
V31	-	-	-	-	-	-	-	5	5	5	5	-	5	5

Key							
-1 < SRRC ≤ -0.6	1	-0.6 < SRRC ≤ -0.4	2	-0.4 < SRRC ≤ -0.2	3	-0.2 < SRRC ≤ -0.1	4
0.1 ≤ SRRC < 0.2	5	0.2 ≤ SRRC < 0.4	6	0.4 ≤ SRRC < 0.6	7	0.6 ≤ SRRC < 1	8

3.2. Sensitive parameters

The identification of more sensitive parameters was carried out independently for each output parameter in all selected locations. SRRC, which is a coefficient between −1 and 1, was selected for this purpose. The positive SRRC indicates that the input parameters have a direct relationship with their respective output parameter while the negative SRRC indicates an inverse relationship between input parameters and their respective output parameters. More specific investigation of sensitivities, as well as the similarities among different locations, are investigated in the following sections.

Table 4 illustrates the more sensitive parameters with their associated

Table 5
SRRC of sensitive input parameter for TDH in (a)Living room, (b)Study room and (c)Rumpus room.

	(a) Sensitivity to TDH in Living room								(b) Sensitivity to TDH in Study room								(c) Sensitivity to TDH in Rumpus room							
Input	*Aw*	*BWh*	*Cfa*(B)	*Csa*	*Cfa*(S)	*BSk*	*Cfb*(M)	*Cfb*(H)	*Aw*	*BWh*	*Cfa*(B)	*Csa*	*Cfa*(S)	*BSk*	*Cfb*(M)	*Cfb*(H)	*Aw*	*BWh*	*Cfa*(B)	*Csa*	*Cfa*(S)	*BSk*	*Cfb*(M)	*Cfb*(H)
V3	-	4	4	4	-	4	-	-	4	3	3	4	3	4	-	4	-	4	4	4	4	-	-	-
V4	-	-	-	-	-	-	-	-	5	5	6	5	5	5	-	-	-	5	5	5	5	-	-	-
V5	-	-	-	-	-	-	-	-	4	-	4	-		-	4	4	-	-	-	-	-	-	-	-
V9	-	-	-	-	-	-	-	-	-	-	-	-	-	-	-	-	4	4	4	-	-	-	-	-
V11	-	-	-	-	-	-	-	-	-	5	-	-	-	-	-	-	3	-	-	-	-	-	-	-
V16	2	6	6	7	7	7	7	7	-	5	5	5	5	5	5	5	-	-	-	-	-	-	-	-
V17	-	-	-	-	-	-	-	-	3	5	-	6	6	6	6	6	-	-	-	-	-	-	-	-
V19	-	-	-	-	-	-	-	-	3	5	-	6	6	6	6	6	-	-	-	-	-	-	-	-
V20	-	-	-	-	-	-	-	-	-	-	-	-	-	-	-	-	3	6	6	6	6	6	6	6
V24	3	-	-	5	5	5	6	6	-	-	-	-	-	-	-	-	3	5	5	6	6	6	6	6
V25	-	-	4	-	-	-	-	-	3	-	4	-	-	-	-	-	-	-	-	-	-	-	-	-
V27	-	-	-	-	-	-	-	-	3	-	4	5	5	-	5	5	-	-	-	-	-	-	-	-
V28	-	-	-	-	-	-	-	-	6	-	-	4	4	4	3	3	7	2	3	2	2	2	2	2
V31	-	4	-	-	-	-	-	-	7	3	-	2	2	2	2	2	-	-	-	-	-	-	-	-

Key: -1 < SRRC ≤ -0.6 (1); -0.6 < SRRC ≤ -0.4 (2); -0.4 < SRRC ≤ -0.2 (3); -0.2 < SRRC ≤ -0.1 (4); 0.1 ≤ SRRC < 0.2 (5); 0.2 ≤ SRRC < 0.4 (6); 0.4 ≤ SRRC < 0.6 (7); 0.6 ≤ SRRC < 1 (8)

Table 6
SRRC of sensitive input parameter for DUH in (a)Living room, (b)Study room and (c)Rumpus room.

	(a) Sensitivity to TDH in Living room								(b) Sensitivity to TDH in Study room								(c) Sensitivity to TDH in Rumpus room							
Input	*Aw*	*BWh*	*Cfa*(B)	*Csa*	*Cfa*(S)	*BSk*	*Cfb*(M)	*Cfb*(H)	*Aw*	*BWh*	*Cfa*(B)	*Csa*	*Cfa*(S)	*BSk*	*Cfb*(M)	*Cfb*(H)	*Aw*	*BWh*	*Cfa*(B)	*Csa*	*Cfa*(S)	*BSk*	*Cfb*(M)	*Cfb*(H)
V16	-	-	-	-	-	-	-	-	5	5	5	5	5	5	5	5	7	7	7	7	7	7	7	7
V19	-	-	-	-	-	-	-	-	7	7	7	7	7	7	7	7	-	-	-	-	-	-	-	-
V32	1	1	1	1	1	1	1	1	-	-	-	-	-	-	-	-	1	1	1	1	1	1	1	1
V33	3	4	4	4	4	3	4	4	3	3	3	3	3	3	3	3	-	-	-	-	-	-	-	-
V35	-	-	-	-	-	-	-	-	1	1	1	1	1	1	1	1	-	-	-	-	-	-	-	-

Key: -1 < SRRC ≤ -0.6 (1); -0.6 < SRRC ≤ -0.4 (2); -0.4 < SRRC ≤ -0.2 (3); -0.2 < SRRC ≤ -0.1 (4); 0.1 ≤ SRRC < 0.2 (5); 0.2 ≤ SRRC < 0.4 (6); 0.4 ≤ SRRC < 0.6 (7); 0.6 ≤ SRRC < 1 (8)

coefficients regarding annual heating and cooling loads. The ranges are colour-coded to represent the sign and magnitude of the sensitivities. Among 35 input parameters, only the parameters with sensitivity coefficients greater than 0.1 (highlighted in Table 2) are demonstrated in Table 4. Since the magnitude of the maximum sensitivity index was ~ 0.6, the parameters with sensitivities <0.1 (~15% of the maximum sensitivity) are less likely to have a significant impact on the targeted outputs. Table 5 illustrates the SRRC of more sensitive input parameters associated with TDH in Living room, Study room and Rumpus room. Table 6 illustrates the SRRCs of more sensitive input parameters associated with DUH in Living room, Study room and Rumpus room.

3.3. Hierarchical cluster analysis

Since the more sensitive parameters in relation to the targeted outputs show some patterns of similarity among certain locations, HCA was carried out to quantify the levels of similarity among selected locations in terms of the sensitivities of input parameters. Understanding the correlations among the sensitivities in various locations can provide useful information for policymaking and generalised design guidelines. It also can inform the prefabricated construction industry and supply chain on the locations for which similar ranges of envelope solutions could potentially be applied.

The SRRC values of all input parameters were selected as the variables while the locations were selected as label cases. The HCA was carried out for each output parameter separately. In this investigation, the final number of clusters was set as two meaning that the locations will continue to group until they reach two main clusters. However, inside each main cluster, the smaller clusters can indicate more details on a similarity of the building's performance in different locations. In this investigation, the reference number of clusters was set to three or four. This means that if a vertical line was placed on the dendrogram it would intersect four horizontal lines representing four groups. If four group clusters did not occur, three groups were taken as the reference number. Since the more sensitive parameters and their associated coefficients for DUH are very similar for all locations, these parameters were excluded in this section and the HCA focus is on heating and cooling loads and TDH only. Fig. 9 shows the clustering of the locations in relation to each targeted output. Rather than investigating the clusters individually, it is more practical to consider the overall grouping of the locations. Table 7 shows the number of times locations clustered together out of five HCAs (as mentioned in Section 2.5).

4. Discussion

The discussion on the obtained results for baseline performance evaluation, SA and HCA are provided in the following subsections.

4.1. Baseline performance

As shown in Fig. 6, in seven out of eight locations for the selected building the annual cooling load is larger than the annual heating load. The average cooling load of all those locations is 90% higher than that of heating. This may be explained by three characteristics of the building: lightweight construction, well-insulated and airtight envelope and high solar heat gain from large equator-facing windows. These characteristics are also outlined by [17] as the factors that increase the risk of summertime overheating in lightweight buildings. Prefabricated construction due to

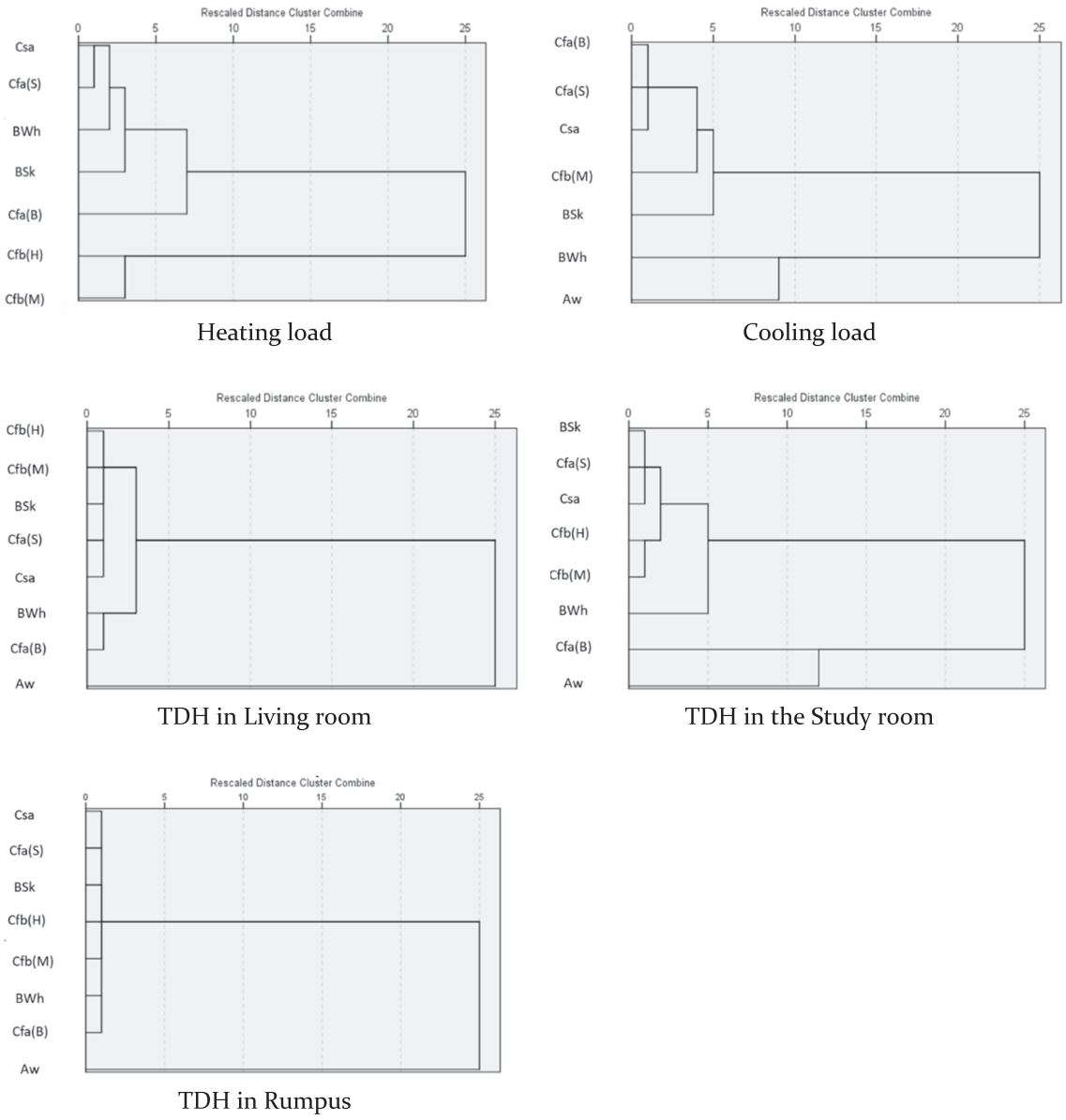

Fig. 9. HCA results for targeted outputs illustrating the groups of locations with similar sensitivities.

Table 7
The number of times locations clustered together in terms of sensitivities to TDH, heating and cooling energy.

Location	Climate	Latitude (° S)	Darwin [*Aw*]	Alice Springs [*BWh*]	Brisbane [*Cfa*]	Perth [*Csa*]	Sydney [*Cfa*]	Mildura [*BSk*]	Melbourne [*Cfb*]	Hobart [*Cfb*]
Darwin	*Aw*	12.4634	–	–	–	–	–	–	–	–
Alice Springs	*BWh*	23.6980	–	–	2	2	2	2	–	–
Brisbane	*Cfa*(B)	27.4698	–	–	–	2	2	–	2	–
Perth	*Csa*	31.9505	–	–	–	–	5	4	4	3
Sydney	*Cfa*(S)	33.8688	–	–	–	–	–	4	4	3
Mildura	*BSk*	34.2080	–	–	–	–	–	–	3	3
Melbourne	*Cfb*(M)	37.8136	–	–	–	–	–	–	–	4
Hobart	*Cfb*(H)	42.8821	–	–	–	–	–	–	–	–

their lightweight nature leads to lower thermal storage in the building increasing the daytime heat gain and risk of overheating in summer. To address this challenge, the exploration of the use of phase change materials as a potentially effective solution is recommended. The overall equivalent infiltration rate of 0.8 ACH, which was found for the building as a result of model calibration (Appendix B) is considered as a high level of airtightness [69]. This together with well-insulated envelope traps the heat indoors causing better thermal performance during winter while increasing the risk of overheating during summer. The large equator-facing windows is another contributing factor which increases the solar eat gain. Another reason for the low amount of annual heating load may be the assumed thermostat settings for heating which is 18 °C and can be considered low if

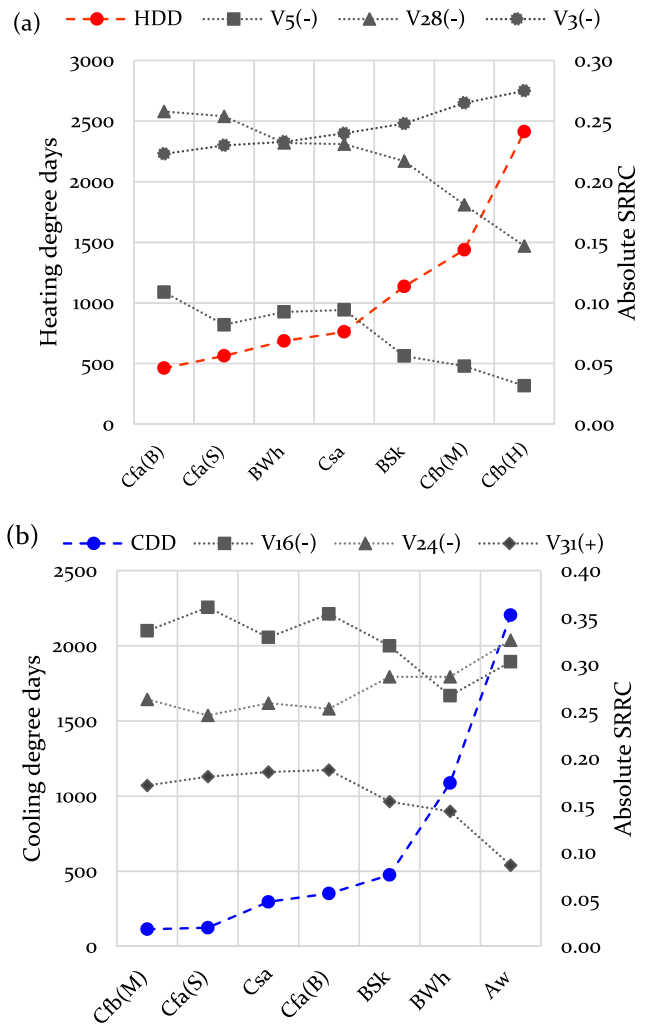

Fig. 10. Parameters that show a relationship between absolute values of sensitivity indices to (a) heating and (b) cooling loads and their respective degree days in selected locations (the signs on the legend demonstrate the actual signs of the sensitivity index).

compared to the heating thermostat settings for living spaces recommended by the Australian Nationwide Energy Rating Scheme (NatHERS) [53].

The fact that the amount of cooling required was found higher than heating in seven out of eight locations, showed that in those locations strategies for reduction of the cooling load should be prioritised. SA can help implement efficient strategies to reduce cooling load by determining more sensitive parameters concerning this indicator. Hobart with an Oceanic climate represents the largest southern latitude (largest distance from the equator) among all other locations and requires heating throughout the year. For this location, the energy efficiency strategies should have a greater focus on the reduction of the heating load.

As can be seen in Fig. 6, smaller values of heating loads (0.1–3 MJ m^{-2}) were observed in four climates: Hot Desert (*BWh*), Humid Subtropical (*Cfa*(B) and (*Cfa*(S)), Savanna (*Aw*) and Hot Summer Mediterranean (*Csa*) which have hot to temperate climates. The maximum annual heating load (90 MJ m^{-2}) was found for Oceanic climate (*Cfb* (H)) which requires heating throughout the year. Also, locations with Oceanic (*Cfb*(M)) and Cold Semi-arid (*BSk*) climates have higher heating loads compared to other climates due to colder winters with values of 33 and 25 MJ m^{-2} respectively. The maximum cooling load among the selected climates is observed in Savanna climate (*Aw*) with 560 MJ m^{-2}. Other climates with high cooling loads are Hot Desert (*BWh*), Humid Subtropical (*Cfa*(B)) with values of 283 and 178 MJ m^{-2} respectively.

As evident in Fig. 6, the cooling load shows an increasing trend with a rise is CDD with exception of Cold Semi-arid (*BSk*) which shows a decrease in heating load compared to Humid Subtropical *Cfa*(B) despite its slightly higher CDD. Also, heating load shows a trend of increase by an increase in HDD, while Cold Semi-arid (*BSk*) climate fails to follow this trend with having higher heating load despite lower HDD compared to Oceanic *Cfb* (M). While this change in trend by Cold Semi-arid (*BSk*) climate is likely related to the dry temperature causing the need for less de-humification in Summer and more humidification in winter (eventuating decrease in cooling load and increase in heating load), further investigations are recommended to study the effects of additional climate factors other than temperature on heating and cooling loads.

In Fig. 7 annual TDH of the Living room, Rumpus and Study room zones are demonstrated. The Living room has large northern (equator-facing) windows while the Study room has west and south-facing windows. The rumpus room also has a north-facing window. Overheating in the Living room, which has large north-facing windows, was found more frequent. This means the level of thermal comfort varies among different spaces in the building. As shown in Fig. 7 among all selected locations the maximum TDH is associated with the living room of the building located in Savanna (*Aw*) with the value of 4,185 h. This value is 40% higher than the TDH of the Study and Rumpus Rooms in the same climate and 48% higher than the average Living room TDH among all selected locations. The high level of summertime TDH may be related to overheating during summer. The reason for overheating could be the high amount of heat gain from large windows as well as a well-insulated airtight envelope with lightweight characteristics [17]. Further overheating in the north-facing zone is more likely to be associated with the solar heat gains from the large windows and a glass door on the north side. This characteristic causes overheating and increased TDH especially in the Savanna (*Aw*) climate which had the highest CDD of all selected locations.

As can be interpreted from Fig. 7 in Oceanic (*Cfb*(H) and *Cfb*(M)), the TDH in the Rumpus room are 29% and 21% higher than average TDH among all locations respectively. In locations with Oceanic (*Cfb*(H)), Oceanic (*Cfb*(M)) and Cold Semi-arid (*BSk*) climates, the TDH in the Rumpus and Study rooms are 29%, 26% and 3% higher than the average TDH among all locations. The fact that these locations have high HDD compared all others may indicate that the TDH in those climates is dominant during the cold season (Fig. 7(b)). By studying the summer and winter TDH, the relationship between HDD, CDD and TDH were investigated. As evident from Fig. 7, the summer and winter TDH has general increasing trends by an increase of CDD and HDD respectively. The exceptions can be seen in Fig. 7(a) where the summer TDH is lower in Cold Semi-arid (*BSk*) and Hot Desert (*BWh*) climates compared to Humid Subtropical (*Cfa*(S)) climate despite their higher CDD. This can be justified given that the TDH is calculated based on PMV which is a function of various factors other than air temperature i.e. mean radiant temperature, relative humidity, air velocity [63]. Therefore, further investigations on the impacts of other climate factors in addition to temperature on TDH is encouraged.

As can be seen in Fig. 7, the Study room TDH during the cold season is greater than the hot season for all selected locations except Savanna (*Aw*) in which the TDH is merely associated with overheating. Also, the winter TDH in Rumpus room outweighs the summer TDH in all climates except Savanna (*Aw*) and Humid Subtropical (*Cfa*(B) and (*Cfa*(S)). This trend of higher winter TDH compared to summer is not repeated for the Living room due to the overheating effect caused by large equator-facing windows.

It is important to note that since the building is conditioned during defined heating and cooling seasons (Table 1), the TDH results are affected by the selected heating and cooling setpoints as also outlined by [29]. However, the selected seasons and setpoints for heating and cooling are the values that are commonly practised in Australia. Although a model setting

with free-running mode throughout the year would eliminate the skewing effect of setpoints on TDH, the current settings in the model represent a more realistic approach. Further investigations on the effects of selected heating and cooling setpoints on the TDH would provide a better insight into the optimal model settings.

The Study room DUH was found to be higher than the other two zones in all locations except Humid Subtropical (*Cfa*(S)) which showed similar DUH for all three zones (Fig. 8). This is because this room does not have a northern (equator-facing) window. The highest DUH among all selected locations is found in Oceanic climates (*Cfb*(H) and *Cfa*(M)) while the minimum DUH was in Humid Subtropical (*Cfa*(B)). The latitude is an important factor in determining the DUH as demonstrated in Fig. 8. While increasing the southern latitude (an increase of distance from the equator), the DUH has a decreasing trend. It is also evident from Fig. 8 that latitude is not the only factor affecting DUH. Another influencing factor is the distance from the standard meridian which affect the amount of daylight during occupied hours. The increase in DUH in Savanna (*Aw*), and Hot Desert (*BWh*) despite smaller southern latitude (closer to the equator) may be due to their greater distance from the standard meridian. This means in those locations the day starts at earlier solar times than others leading to increased DUH, earlier.

By comparing the values obtained for TDH and DUH (Fig. 7 and Fig. 8), it can be observed that TDH are significantly higher than DUH in all climates. The average TDH in Living room, Study room and Rumpus room among all locations were 91%, 90% and 88% greater compared to those of DUH respectively. This reveals that more emphasis on reduction of TDH is required to improve the overall comfort levels in the building.

4.2. Effects of envelope parameters on heating and cooling loads

As evident from Table 4, in all selected climate zones the building's annual heating load is most influenced by three parameters: the thickness of external wall insulation, north-facing window shading factor and north-facing window area. Factors related to the roof insulation, north-facing shading and south-facing window type are other sensitive parameters impacting heating load. Furthermore, the thickness of the wall's interior layer was found sensitive in regard to heating load, since an increase in this layer would result in greater thermal insulation. The range of the thermal conductivities of external wall and roof insulation materials used for prefabricated components is small (0.022–0.040 W m^{-1} K^{-1}) [39]. Therefore the thermal resistance of the wall (consequently effect on heating load) mainly dependent on the thickness of the insulation. It is also apparent that the effects of north facing window areas and their shadings are dominant parameters for southern hemisphere. The interior layer of external walls has thickness between 5 and 100 mm which is a wide variation compared to the specific heat (0.4–1.1 kJ $kg^{-1}K^{-1}$). As such, the thermal mass of the wall is impacted more by the thickness than the specific heat. A general conclusion is that the thermal mass characteristics of the interior layer of the walls are sensitive to heating load.

The signs and levels of sensitivities among selected climates regarding heating load did not show significant variations for most parameters. However, the parameters which show a trend of change among locations were investigated further as shown in Fig. 10(a). As the HDD increases, the sensitivity of insulation thickness increases. This is justifiable since the locations with higher HDD require more insulation to effectively reduce the heating load. On the other hand, the north-facing window area and the wall's interior finish have an opposite effect on the level of sensitivities with an increase of HDD. This means that the solar heat gain and thermal mass have less impact on reducing heating loads in the climates with high HDD. The reason could be the large amount of heating load in those climates which is more challenging to minimise compared to the climates with low HDD.

The most sensitive parameters for cooling load were north-facing window: shading factor, type and area. In addition, factors related to the south, east and west-facing windows were found to be amongst most sensitive parameters for the cooling load (Table 4). The cooling load is largely affected by the amount of solar heat gain especially from north side in southern hemisphere. The range of shading factor on the windows is between 0% and 60%. The shading factor and the area have a major effect on the amount of solar heat gain from the windows, making these parameters most sensitive in regards to cooling load.

Some parameters showed an increasing trend when mapped to CDD (Fig. 10(b)). The level of sensitivity to north-facing windows' type increase in climates with higher CDD. This indicates that the type of window is an important factor in the cooling dominated climates. The negative sign of SRRC related to window type shows that the increase in window ID number (increase in insulation) reduces the cooling load. Also, it was found that the sensitivities to north-facing window shading factor decrease while the CDD increase which is an indicator that this factor is not as effective for warmer climates. This is justifiable considering that minimising greater amounts of cooling load is more challenging and therefore certain strategies may appear less impactful compared to the climates with less cooling requirements. It is important to note that the effectiveness of input parameters is measured by the rate of change in the output parameter. Therefore, the greater the magnitude of the output parameter, the smaller the reduction impact would appear. Therefore, the sensitivity trends and the impact of input parameters should be assessed by considering the magnitude of the corresponding output parameter. Unlike the parameters shown in Fig. 10, other parameters did not show a particular trend or relationship to HDD or CDD. Further analysis through HCA provides more details on the similarity of the response in different groups of locations.

Another important issue is that heating and cooling loads are both affected by north window shading factor and north window area however in opposite directions. This finding aligns with [24] which highlighted the important role of windows' parameters on the building's energy performance. The opposite directions of sensitivities indicate that increasing these parameters can affect one output positively while affecting the other negatively. To address the counteracting effects of window parameters of multiple targeted outputs the use of reconfigurable solutions such as electrochromic or thermochromic glazing can be explored in future research. For further investigation, the effect of both parameters i.e. total energy consumption for heating and cooling was considered as a targeted output in an optimisation study [40].

The study focuses on prefabricated components documented in the data set [39], majority of them are lightweight. This implies that the energy consumption sensitivities found for prefabricated components may also applied for lightweight buildings with low thermal mass. Furthermore, some investigated envelope characteristics such as shading factor and window size are applicable to all types of buildings and therefore they are likely to be similarly sensitive in other building types, noting that their relative importance levels may vary depending on the ranges of characteristics in other envelope parameters.

4.3. Effects of envelope parameters on thermal discomfort hours

As evident in Table 4, the more sensitive parameters to TDH in the Living room are north windows' type and shading factor. North window parameters are among the most sensitive factors in relation to Rumpus room TDH. Also, wall and roof insulation are found to have an impact on TDH in the Rumpus room. Factors related to the south and west-facing windows were found to have the highest impact on TDH in the Study room. This is justifiable since this room has windows facing those directions. Similar to heating and cooling load, the effect of window parameters and shading factor on TDH especially on north side (dominant solar gain façade in southern hemisphere) is notable.

Other sensitive parameters are found to be wall insulation and the interior finish thickness, which is similar to the results of SA for the heating load. Since the range of thermal conductivities for insulation materials is small, the thermal resistance of the wall is directly proportionate to the thickness of insulation. Similar to the reasons for the sensitivity of heating and cooling load the thickness of the insulation and

thermal mass characteristics are the sensitive parameters for TDH.

The higher sensitivity of window parameters and insulation to thermal comfort is in line with the findings of [27] and [29].The signs of SRRC in regard to TDH agree in most of the locations while the results for some parameters in Savanna (*Aw*) and Humid Subtropical (*Cfa*(B)) climates show a sensitivity sign opposite to other locations. These parameters are the factors associated with the north-facing window such as window area, type and shading for Savanna (*Aw*) and window type and west window type in Humid Subtropical (*Cfa*(B)). The frequent difference in the sign of sensitivities in Savanna (*Aw*) climate is due to the hot climate that requires cooling year-round. While other climates benefit from heat gain from larger windows and smaller shading in the cold season, Savanna (*Aw*) climate requires minimisation of heat gain through smaller windows and increased shading strategies. In addition to the signs, the levels of sensitivity also varied among selected climates in regard to TDH. Certain parameters show higher sensitivities to TDH in some climates compared to others.

The north-facing window shows lower sensitivity to TDH in the living room in Hot Desert (*BWh*) and Humid Subtropical (*Cfa*(B)). Instead, TDH in same climates together with Humid Subtropical (*Cfa*(S)) show higher sensitivity to insulation thickness of walls. This means increasing the insulation of walls has more impact on improving thermal comfort compared to other climates. On the other hand, the maximisation of the north window area seems to be more important in Oceanic (*Cfb*(M) and *Cfa*(H)) compared to other climates. This is justifiable since the oceanic climates have colder weather and benefit from solar heat gain through north-facing windows.

Although the sign and levels of sensitivities largely vary among climate zones, no specific relationship was found between HDD, CDD and sensitivities to TDH. This means that the decisions on envelope parameters should consider the level and sign of sensitivities in individual climates while necessitates further investigation through conducting multi-objective optimisation for each specific location.

4.4. Effects of envelope parameters on daylight unsatisfied hours

According to the results of SA, the more sensitive parameters for DUH in different spaces are associated with visual transmittance and shading factor on different orientations of the building depending on the selected room. For instance, since the Living room has south and north-facing windows, the factors associated with those orientations are found to be the more sensitive parameters. Similarly, south and west parameters were found to be sensitive for Study room DUH and the north parameters for the Rumpus room DUH. Although the Living room has north and south-facing windows, the shading factor of these orientations was not found sensitive for DUH of this space. This may be due to the large north-facing windows and glass doors in the Living room that provides sufficient daylight even with high levels of shading factors. The range of visual transmittance is 10–90% while that of shading factor is 0–60% [39]. The large variations of those inputs lead to significant impact on the amount of daylight received in indoor spaces. This justifies the high sensitivity levels obtained for those parameters.

The importance of window selection on the visual comfort aligns with the findings of [25].

The identification of more sensitive parameters for the selected building targeting energy consumption, TDH and DUH reveal that different input parameters affect two or several output variables in opposite directions. For instance, an increase in north-facing window shading factor results in an increase of TDH in the Living room while decreasing the cooling load. This indicates the need for further investigation through multi-objective optimisation to find possible optimised solutions.

Throughout Sections 4.1, 4.2, 4.3 and 4.4. an attempt was made to explain the causes and rationale behind the baseline performance as well as signs and sensitivities of certain input variables in respect to output parameters. Understanding those functions can lead to more in-depth insight into buildings' behaviour under various climatic conditions and their corresponding design responses. As such, the global application of this research does not lie in the sensitivity results themselves but in the realisation of those underlying functions in each climatic condition and the appropriate design responses to address them.

4.5. HCA analysis

The HCA was carried out to better understand the similarity of sensitivities among eight selected locations in Australia. The clusters shown in Fig. 9 are further discussed in this section. The clusters formed in HCA analysis are indicative of the similarities of sensitive parameters and their values among the selected climates. The HCA analysis heating load results show that the two locations in Oceanic climate share a cluster, Humid Subtropical (*Cfa*(B)) forms an individual cluster while other remaining climates are grouped in a third cluster. For cooling load, Hot Desert (*BWh*) and Humid Subtropical (*Cfa*(B)) form one cluster while Savanna (*Aw*) is clustered separately, and other remaining climates share another cluster.

In relation to the TDH, the group of Humid Subtropical (*Cfa*(S)), hot summer Mediterranean (*Csa*), Cold Semi-arid (*BSk*) and Oceanic (*Cfb*(H) and *Cfb*(M)) climates appear to have similar performance while Savanna (*Aw*), Humid Subtropical (*Cfa*(B)) and Hot Desert (*BWh*) are in different clusters either as individual group or groups of two.

Humid Subtropical (*Cfa*(S)) and Hot Summer Mediterranean (*Csa*) clustered together in all five clustering analysis while these two locations grouped with Cold Semi-arid climate (*BSk*) four times. The clustering of these three locations despite different climates can be a result of their similar southern latitudes. The two locations with Oceanic climate (*Cfb*(H) and *Cfb*(M)) grouped four times. Also, Oceanic (*Cfb*(M)) and Cold Semi-arid (*BSk*) have similar performance for all outputs except heating load. Hot Desert (*BWh*), Humid Subtropical (*Cfa*(B)) and Savanna (*Aw*) seemed not to be clustering well while each of them has clustered one or two times with other locations.

The similarities in sensitivity among selected locations can be useful in developing generalised national and international guidelines, policies or high-level minimum requirements to be used in concept design stage where initial debates on potential design decisions are made. Examples of this generalised approach is the minimum required standards provided by NCC [38] in Australia which provides recommendations for groups of locations e.g. minimum R-value of wall and roof is provided for a group of climates. While the generalised approach can be useful in concept designs stage, the later stages would require more personalised approaches using the accurate climate data to estimate the building's performance in each specific location. Further application of the location groups in regard to environmental design requirements would be to inform prefabrication industry and supply chain on locations for which similar ranges of envelope solutions could potentially be applied and lead to classification and standardisation of their products based on locations.

4.6. Limitations and future research opportunities

This article presents the results and findings of baseline performance evaluation and sensitivity analysis of a single-family residential building. The input parameters selected for this study are limited to the envelope components while other factors are considered fixed. The effects of other contributing factors such as buildings' spatial design and geometry, temperature setpoints, occupancy schedules, natural ventilation and air change rates are not considered in this investigation. Since this article presents a specific building with certain assumptions, the generated results cannot be generalised, instead the critical analysis to investigate the underlying functions behind the performance responses and the design recommendations to improve building's behaviour can be used across ranges of lightweight prefabricated projects.

The weather files used in the simulations are Typical Meteorological Year (TMY) that represents long term averages of the weather data. However, TMY data files cannot foresee climate change effects in the

coming years. Therefore, the consideration of climate change effects is recommended for future research in order to generate more realistic outcomes.

The lightweight characteristic of prefabricated components reduces the thermal mass effect leading to higher temperature fluctuations and reduced thermal comfort compared to heavy-weight traditional buildings. Exploration of the use of innovative technologies such as phase change materials as a potentially effective solution in prefabricated buildings is recommended for future research. Also, to address the counteracting effects of window parameters of multiple performance parameters the use of reconfigurable solutions such as electrochromic or thermochromic glazing can be explored in future research.

5. Conclusions

In this article, a regression-based global sensitivity analysis (SA) was implemented to investigate the effects of building envelope parameters on cooling and heating loads as well as thermal discomfort hours (TDH) and daylight unsatisfied hours (DUH) of a prefabricated house in six climate zones. The input variables are envelope parameters that can be applied in lightweight prefabricated construction. TRNSYS was used for the house's cooling and heating load estimations. Daylighting simulations were performed by using DAYSIM and Radiance. jEPlus and SimLab were used to perform parametric runs and SA respectively. The most sensitive input parameters were obtained for all eight locations. Also, to find similar patterns of sensitivity in different climate zones, a hierarchical cluster analysis (HCA) was carried out. According to the findings of this study, the following conclusions were drawn:

The cooling loads were larger than the heating loads (up to 90%) in seven of eight locations. This may be explained by three characteristics of the building: lightweight construction, airtight envelope and high solar heat gain from large northern (equator-facing) windows. Prefabricated construction due to their lightweight nature leads to lower thermal storage in the building increasing the daytime heat gain and risk of overheating in summer. As such, prioritising the strategies to reduce cooling load would lead to achieving better overall energy performance. Exploration of the use of phase change materials as a potentially effective solution in prefabricated buildings is recommended. Also, TDH was found significantly higher than DUH in all climates (up to 91%). This means more emphasis on reduction of TDH is required to improve the overall comfort levels in all climate zones investigated.

The highest Living room's TDH was observed in the Savanna climate where the TDH was 48% higher than the average Living room's TDH among all selected locations. In Oceanic climates, the TDHs of the Rumpus and Study rooms were up to 29% greater than the corresponding average TDH among all selected locations. The TDH of Study and Rumpus rooms were more dominant during the heating season in all climate zones except Savanna where the TDH was associated with overheating during cooling seasons. This is likely to be related to the assumed winter setpoint (18 °C) which may be considered low. Overheating in the Living room, which has large equator-facing windows, was more frequent. This means the level of thermal comfort varies among different spaces in the building. Although the level of DUH decreases with increase in latitude (increased distance from the equator), the locations with greater distance from standard meridian were found to have greater DUH despite being closer to the equator.

The sensitivity analysis revealed the important focus areas in various climatic conditions. Window glazing and shading were found among the most influential parameters in respect to all targeted outputs. Some parameters show a relationship between their sensitivity levels to heating and cooling load and their corresponding degree days in various climates. These trends indicate that the type of window has a higher impact on the reduction of cooling load in the cooling dominated climates while insulation of wall was found a more effective strategy in heating-dominated climates.

The rationale behind baseline performance, the sensitivities of certain input variables and the trends of sensitivity against degree days as outlined in the discussion, can lead to a more in-depth understanding of buildings' behaviour under various climatic conditions and their corresponding design responses. This insight into the underlying functions and the design responses can be incorporated during early design stages by practitioners across ranges of projects.

The findings from SA implied the need for conducting multi-objective optimisation. Firstly, climate conditions significantly change the sensitivities of building envelope variables on performance parameters. Although the sensitivity levels of heating and cooling loads showed some patterns depending on HDD and CDD, no specific relationship was found between HDD, CDD and sensitivities to TDH. Secondly, by comparing the sensitivity parameters among performance parameters it was found that some envelope variables affect two or more performance parameters in the opposite directions.

The HCA results reveal that Humid Subtropical (Sydney), Hot Summer Mediterranean (Perth) have similar performance in terms of sensitivity parameters for all outputs. Oceanic (Melbourne) and Cold Semi-arid (Mildura) climates have similar performance for all outputs except heating load. Also, the two locations with Oceanic climates (Hobart and Melbourne) show similar performances for all outputs except cooling load. The similarities in sensitivity among selected locations can be useful in developing generalised guidelines, policies or minimum required standards to be used in concept design stages. Also, it can inform the prefabrication industry and supply chain on locations where similar ranges of envelope solutions could be applied leading to classification and standardisation of their products based on locations.

The methods used for conducting SA in this study as well as the critical analysis on the causes of sensitivity performances and corresponding design responses can be used by the design practitioners and decision-makers across a diverse range of prefabricated building projects. As such, the global application of this research does not lie in the sensitivity results themselves but in the realisation of those underlying functions in each climatic condition and the appropriate design responses to address them. The research outcomes derived from the six climate zones selected in Australian contexts may apply to new and retrofit housing design upgrades in the similar climates outside Australia. Even so, the applicability beyond Australian contexts requires further extensive studies for the justification due to not only building regulation differences but the cultural ones that to some extent affect building design materials, systems and configurations. Accordingly, the universality of this study's findings outside Australian contexts can be considered as an opportunity of further research exploration.

CRediT authorship contribution statement

Sareh Naji: Methodology, Software, Validation, Formal analysis, Investigation, Data curation, Writing - original draft, Writing - review & editing, Visualization. **Lu Aye:** Conceptualization, Methodology, Software, Validation, Resources, Data curation, Writing - review & editing, Visualization, Supervision, Project administration, Funding acquisition. **Masa Noguchi:** Supervision, Writing - review & editing.

Declaration of Competing Interest

The authors declare that they have no known competing financial interests or personal relationships that could have appeared to influence the work reported in this article.

Acknowledgements

This research was conducted within the Department of Infrastructure Engineering as a part of PhD thesis of Sareh Naji, who has been supported by Melbourne Research Scholarship. This work was co-funded by the ARC Centre for Advanced Manufacturing of Prefabricated Housing [ARC Grant IC150100023]. The authors would like to acknowledge the

cooperation and assistance of the residents of the house. The supports and helps of Habitech Systems are also gratefully acknowledged. Thanks are also due to Oskar Casasayas (Deakin University) for proofreading the submitted version of the manuscript.

Appendix A:. The features of the selected locations and the case building

See Figs. A1-A4 and Tables A1-A3.

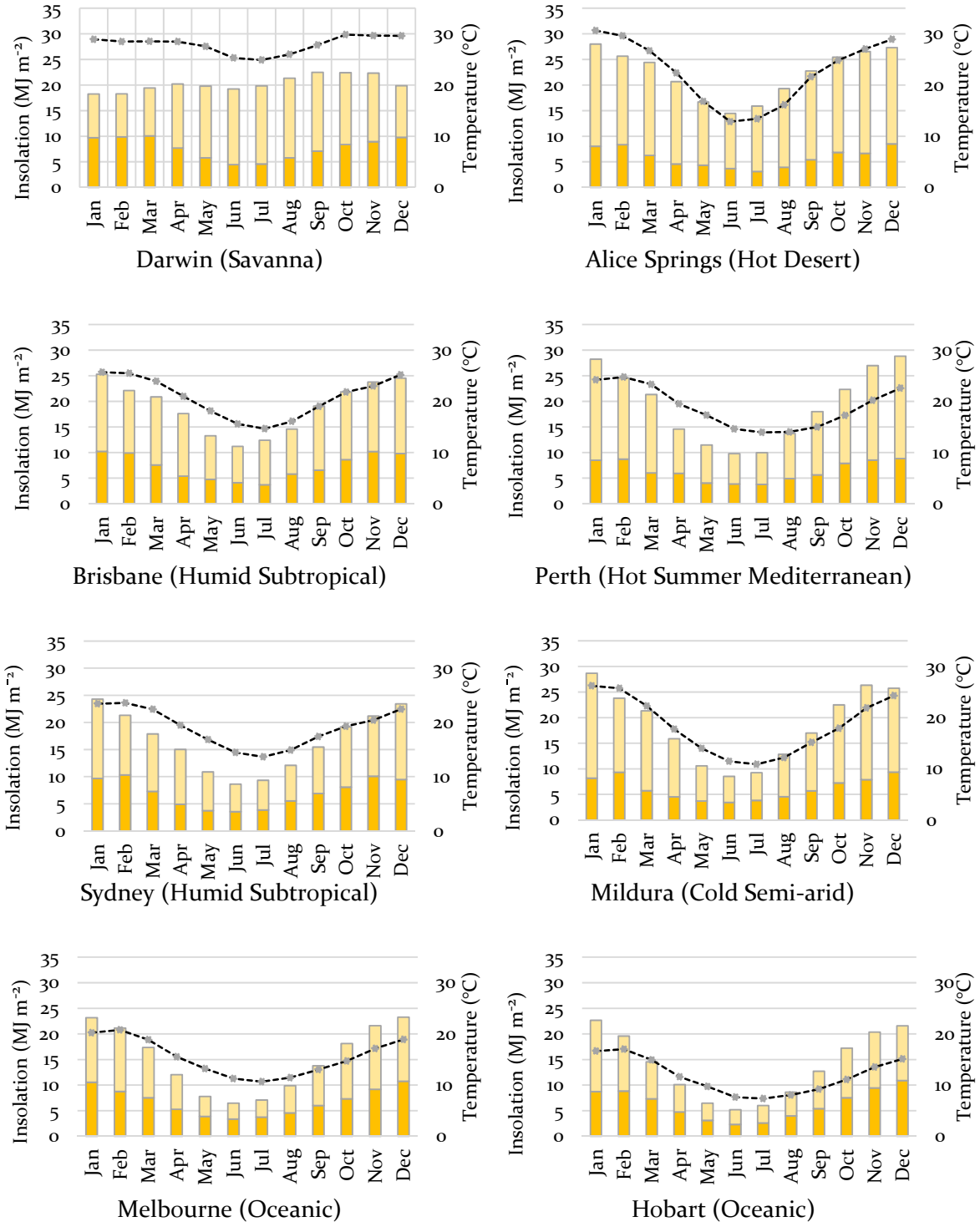

Fig. A1. Monthly average daily solar radiations (diffuse: darker colour, total: stacked column) received on the horizontal plane and monthly average ambient air temperatures.

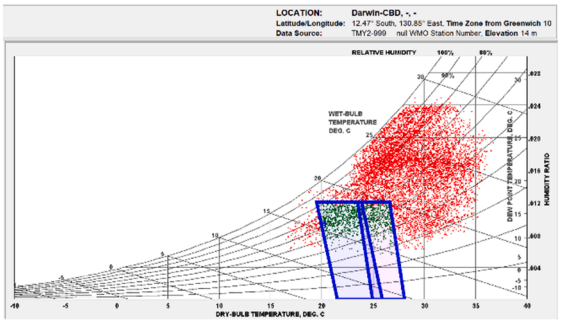

Darwin (Savanna)

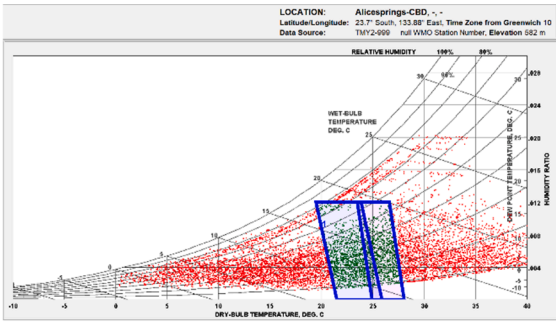

Alice Springs (Hot Desert)

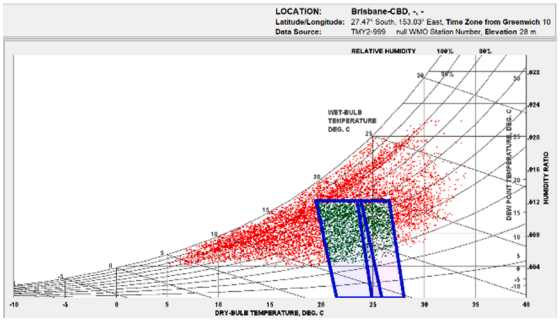

Brisbane (Humid Subtropical)

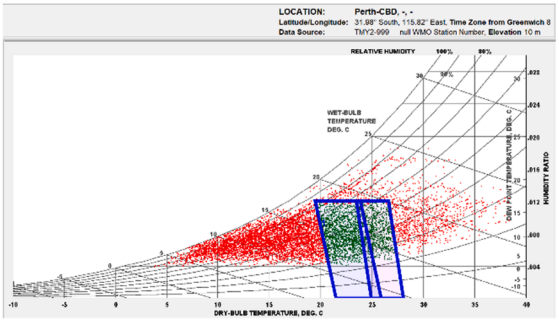

Perth (Hot Summer Mediterranean)

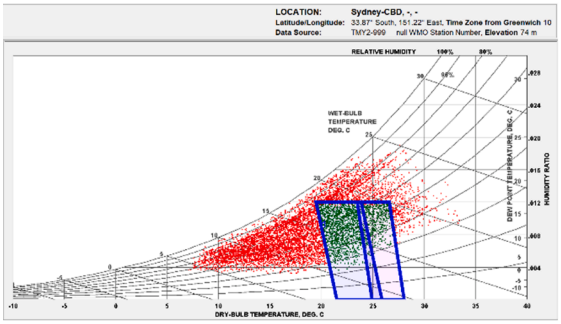

Sydney (Humid Subtropical)

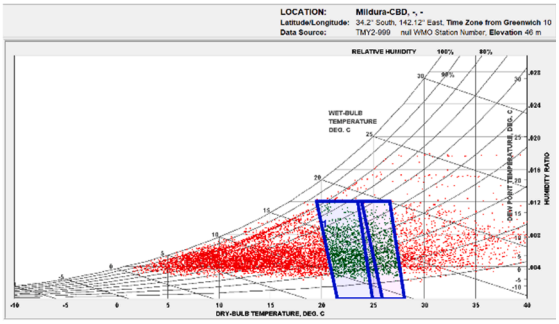

Mildura (Cold Semi-arid)

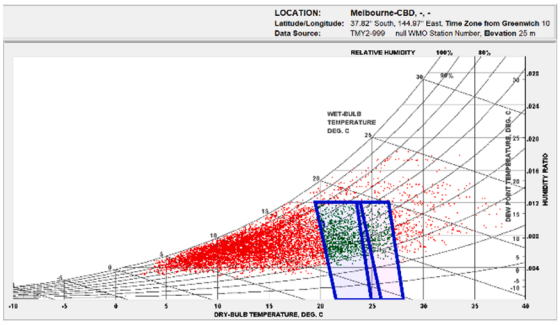

Melbourne (Oceanic)

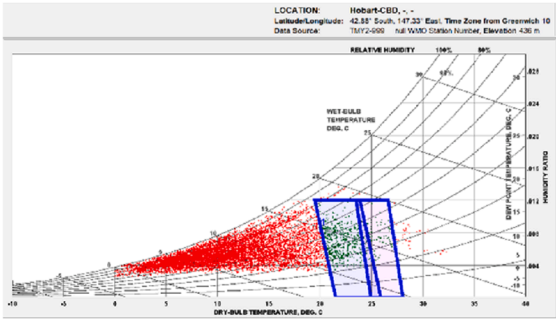

Hobart (Oceanic)

Fig. A2. Psychometric charts (generated with Climate Consultant 6.0 (Liggett and Milne, 2020) [49]).

Fig. A3. The images of the selected building located in Melbourne, Australia: (a), (b), (c) under construction and (d), (e) completed [52].

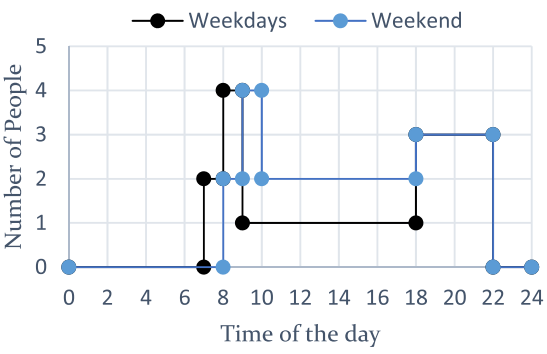

Occupancy- Living room

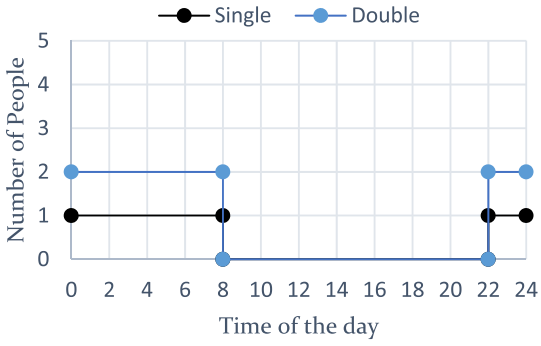

Occupancy- Bedrooms

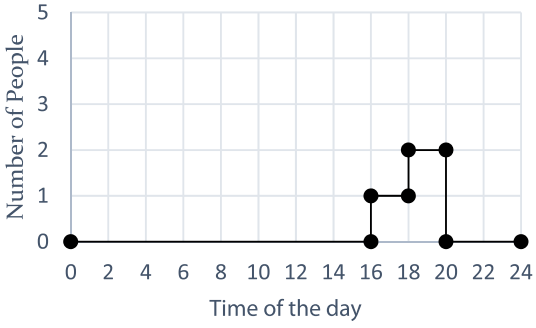

Occupancy- Rumpus room

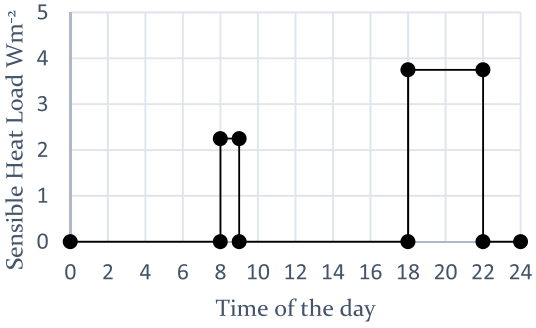

Lighting- Living room/Rumpus room

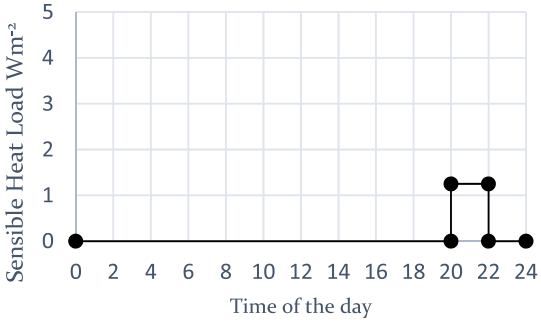

Lighting- Bedrooms

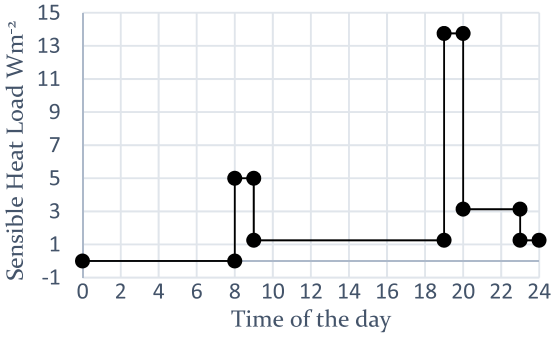

Appliances-Living room

Fig. A4. Schedules used in the simulation of the selected building.

Table A1
Features of the selected locations.

Climate Code*	NCC Zone	City	Population ('000)	Location	WMO Station No.
Aw	1	Darwin	118.4	12.4634° S, 130.8456° E	94120
Bwh	3	Alice Springs	23.7	23.6980° S, 133.8807° E	94326
Cfa(B)	2	Brisbane	2,270.8	27.4698° S, 153.0251° E	94578
Csa	5	Perth	1,671.0	31.9505° S, 115.8605° E	94610
Cfa(S)	5	Sydney	4,824.0	33.8688° S, 151.2093° E	94767
BSk	4	Mildura	32.7	34.2080° S, 142.1246° E	94693
Cfb(M)	6	Melbourne	4,485.2	37.8136° S, 144.9631° E	94866
Cfb(H)	7	Hobart	222.3	42.8821° S, 147.3272° E	94975

Table A2
The properties of thermal zones in the selected building.

Thermal Zone	Area (m^2)	Volume (m^3)	Glazing area (m^2)	Glazing to floor area ratio
Living/dining	80.99	242.96	35.85	0.442
Study	16.70	50.10	4.26	0.255
Bed1	26.42	68.69	7.64	0.289
Bed2	16.17	45.58	5.33	0.329
Bed3	15.51	43.50	2.47	0.159
Bed4	16.77	47.28	3.70	0.220
Rumpus	12.21	34.24	2.47	0.202
Bathroom1	4.00	11.20	0.79	0.197
Bathroon2	5.58	15.62	0.94	0.168
Bathroom3	8.91	24.94	2.47	0.277

Table A3
The materials used in the construction of the selected building (baseline).

Component	Material	Thickness (mm)	Conductivity ($Wm^{-1}K^{-1}$)	Density ($kg\ m^{-3}$)	Specific Heat ($kJ\ kg^{-1}K^{-1}$)	Resistance ($m^2\ K\ W^{-1}$)	Reference
Exterior Wall	Mag board	9	0.450	1000	0.880	–	[70]
	EPS core	149	0.036	25	1.250	–	[71]
	Plywood	12	0.150	800	1.200	–	TRNSYS Layer Library
Interior Wall	Plasterboard	10	0.190	1300	0.840	–	[72]
	Timber stud	90	1.300	33	1.024	–	TRNSYS Layer Library
	Airspace	90	–	–	–	0.18	[73]
	Plasterboard	10	0.190	650	0.840	–	[72]
Floor	Concrete	150	1.130	1400	1.000	–	TRNSYS Layer Library
	**Ceramic tiles	15	1.300	2300	0.840	–	[74]
	**Carpet	20	0.060	288	1.380	–	TRNSYS Layer Library
Ceiling	Plasterboard	10	0.190	1300	0.840	–	[72]
	Timber veneer	35	0.130	600	2.000	–	TRNSYS Layer Library
	Airspace	530	–	–	–	0.16	[73]
	Particle board	20	0.056	300	1.000	–	TRNSYS Layer Library
	Carpet	20	0.060	288	1.380	–	TRNSYS Layer Library
Roof	Steel	1	15.000	7800	1.800	–	TRNSYS Layer Library
	Airspace	37	–	–	–	0.17	[73]
	EPS	150	41.380	0.13	25.000	–	[71]
	Airspace	530	–	–	–	0.16	[73]
	Timber veneer	35	0.130	600	2.000	–	TRNSYS Layer Library
	Plasterboard	10	0.190	1300	0.840	–	[72]
Glazing	ID: 201	(the properties are specified in Table 3)					

** Ceramic tiles are used for the wet areas while the carpet is used for the other spaces

Appendix B:. Calibration and validation of the building model

B.1. Method

Table B1
The equipment used for monitoring the selected building.

Item	Model	Manufacturer	Quantity
USB temperature data logger	RC-5	Elitech	2
Temperature & RH data logger	UX100-003	Onset	3

Table B3
R^2, RMSE, MBE, MAE and CC for various zones for the validation period (15:00 on 30March 2018–00:00 on 2 April 2018).

Zone	R^2	RMSE (°C)	MBE (°C)	MAE (°C)	CC
Living	0.92	1.20	1.13	1.13	0.96
Bed1	0.93	0.64	0.47	0.48	0.96
Bed3	0.93	1.15	−1.08	1.08	0.96
Bed4	0.86	0.93	0.77	0.77	0.93

Table B2
R^2, RMSE, MBE, MAE and CC for various infiltration rates (between 15:00 on 30 March 2018 and 19:00 on 31 March 2018).

Infiltration rate (ACH)	R^2	RMSE (°C)	MBE (°C)	MAE (°C)	CC
0.6	0.80	1.27	0.88	1.09	0.90
0.7	0.80	1.16	0.71	0.97	0.90
0.8	0.87	1.07	0.75	0.88	0.93
0.9	0.80	1.00	0.39	0.77	0.90
1.0	0.80	0.96	0.24	0.72	0.90

The baseline building model was calibrated and validated by comparing the simulated and measured indoor temperatures of four zones (Living, Bed1, Bed3, and Bed4) in different periods. The details on the building location and characteristics are provided in Section 2.1.2. The details of the measuring devices applied are presented in Table B1. One 'Elitech' logger (with 30 min recording interval) was placed to measure the outdoor air temperature in a shaded area outside the building. Another 'Elitech' logger (with 30 min recording interval) was used in Bed3. Three 'Onset' loggers (with 5 min recording interval) were used in three zones: Living, Bed1 and Bed4 (Fig. 3).

For comparing the indoor measured and simulated temperature values of the selected building, the realistic weather data for that specific period of time was required. For this reason, the weather and solar radiation data were acquired from the Bureau of Meteorology (BOM) for

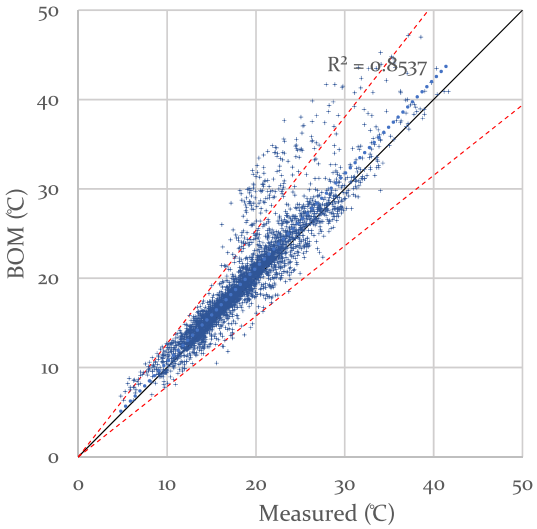

Fig. B1. Scatter plot: measured vs. BOM ambient air temperature.

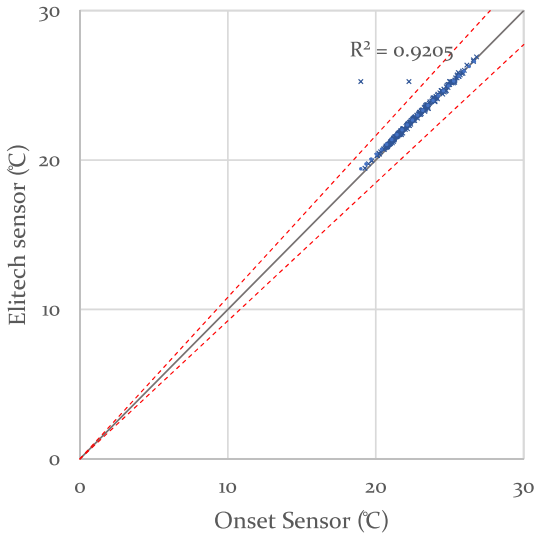

Fig. B2. Scatter plot: measured indoor temperature in the living room using two different sensors.

this specified period. Since those data were obtained in 1-minute intervals, the values were aggregated and converted to 1-hour intervals. TRNSYS Type99 [75] was used for reading and processing of the customised weather data. The data include dry bulb temperature, relative humidity, and total solar radiation on a horizontal surface.

In order to check the accuracy of the data loggers, two different evaluation was carried out. First, the data acquired from the outdoor temperature sensor were compared to the data obtained from BOM. Second, the temperature data from two different sensors in the same room were compared.

The materials used in the building and their properties were defined in the model. To reduce the uncertainty of occupants, lightings and internal appliances heat gain schedules, and air-conditioning system operations, an unoccupied period (30 March −2 April 2018) was selected for calibration and validation. The single unknown air infiltration rate was calibrated using the measured data between 15:00 on 30 March 2019 and 19:00 on 31 March 2018. The validation was carried out for the period between 19:00 on 31 March 2018 and 00:00 on 2 April 2018. Coefficient of determination (R2), Root Mean Square Error (RMSE), Mean Bias Error (MBE), Mean Absolute Error (MAE) and Correlation Coefficient (CC) were applied for quantifying the agreement between simulated and measured temperatures.

B.2. Results

The measured indoor data were compared with the data from different sources. The outside measured dry-bulb temperatures in the period between 9:00 on 21 December 2017 and 6:00 on 17 May 2018 were compared with the temperature data obtained from BOM and found to have $R^2 = 0.85$, CC = 0.92.

To check the consistency of the data recorded at the loggers, the data from two sensors (one Onset and one Elitech) located in the living room were compared. The comparison between temperatures recorded by two type of data loggers has $R^2 = 0.92$, CC = 0.96, and MBE = 0.2 °C. These results show that the data recorded by the data loggers are accurate enough for validation purpose.

For the calibration of infiltration rate, the simulations were performed for the duration between 15:00 on 30 March 2018 and 19:00 on 31 March 2018 for five infiltration rates. R^2, RMSE, MBE, MAE and CC for the indoor air temperature comparisons (for all Living, Bed1, Bed3 and Bed4) were estimated (Table B2). It was found that the building model with infiltration rate 0.8 ACH has better overall agreement between measured and simulated results. The selected calibrated infiltration rate (0.8 ACH) agrees with the value suggested by Ambrose & Syme [76] (national average value for new residential buildings in Australia).

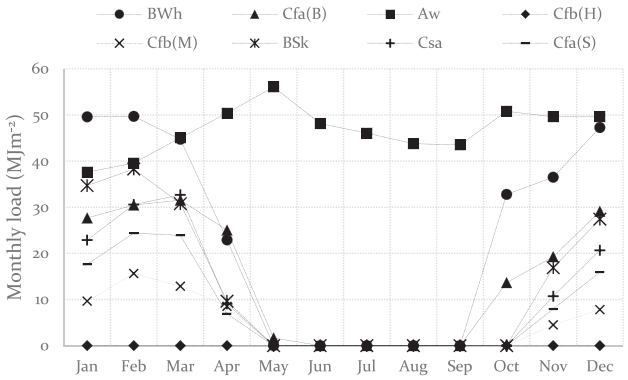

Fig. B3. Scatter plots: measured vs. predicted indoor dry bulb temperatures (19:00 on 1 April 2018–15:00 on 2 April 2018) for various zones.

The scatter plots of the measured versus predicted values of indoor dry bulb temperature during validation period (19:00 on 31 March 2018 – 00:00 on 2 April 2018) for Living, Bed1, Bed3 and Bed4 zones are shown in Fig. B1 in Appendix B. Table B3 presents R^2, RMSE, MBE, MAE and CC for the comparison between measured and predicted indoor temperatures. Better agreements were found for Living and Bed1 zones. The predicted dry bulb temperature values are slightly higher than that of measured in the zones on the ground floor (Living and Bed1). The predicted temperatures in Bed4 are also higher than that of measured, the reverse is true for Bed3. The discrepancies may be attributed by assumed single value infiltration rate for all zones. The dataset for the calibration and validation of the TRNSYS building model is provided in [77]. (see Figs. B2 and B3)

Appendix C:. Supplementary graphs for baseline performance evaluations

The dataset for the baseline performance of the prefabricated house is provided in [78].

See Figs. C1–C4.

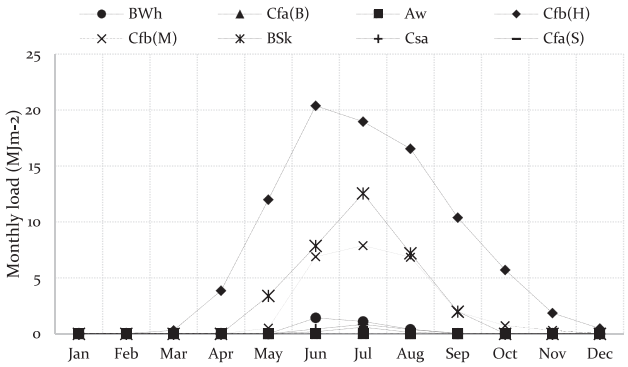

Fig. C1. Baseline monthly cooling loads in all selected locations.

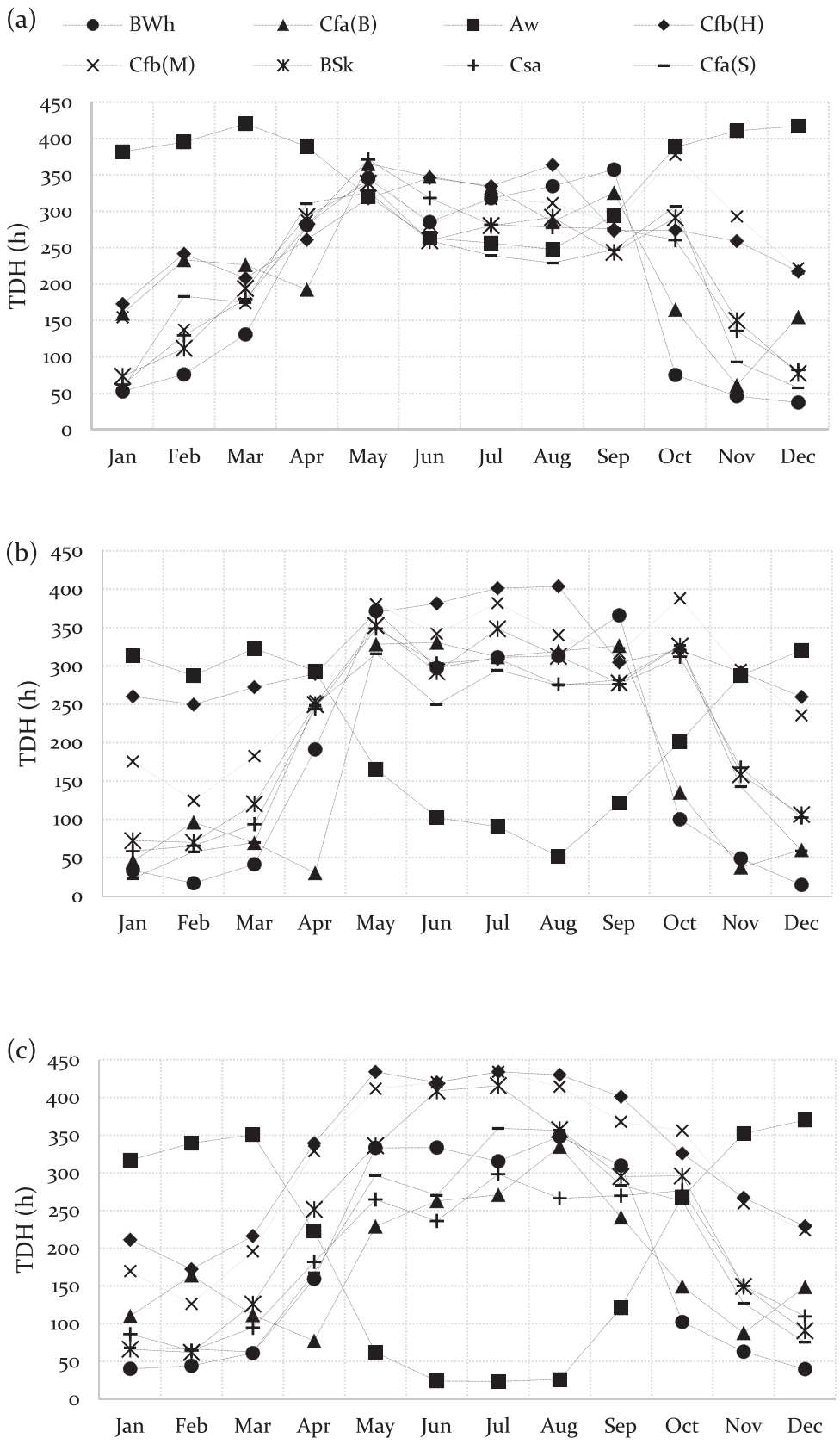

Fig. C2. Baseline monthly heating loads in all selected locations.

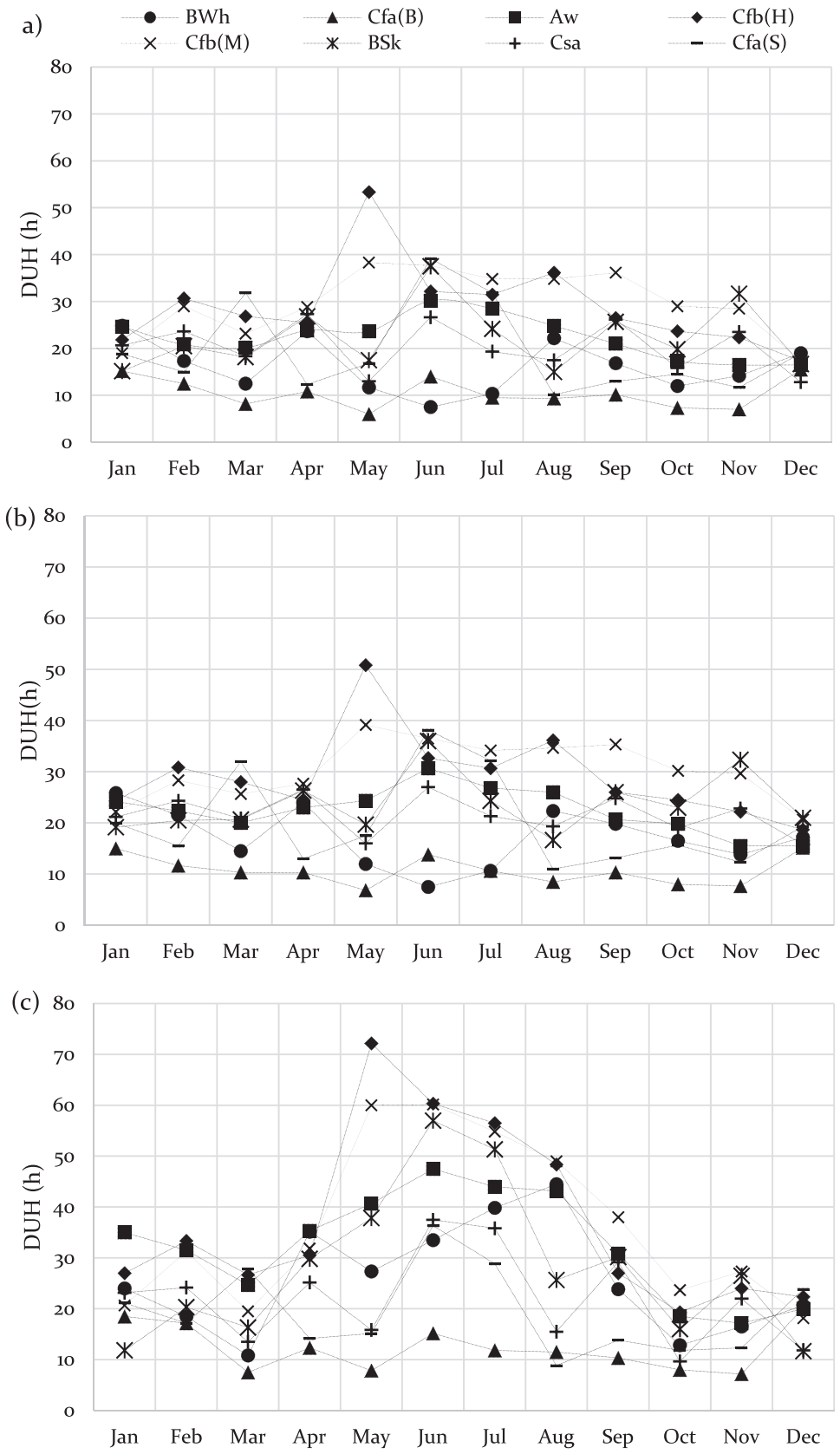

Fig. C3. Baseline monthly TDH in (a) Living room, (b) Rumpus and (c) Study room.

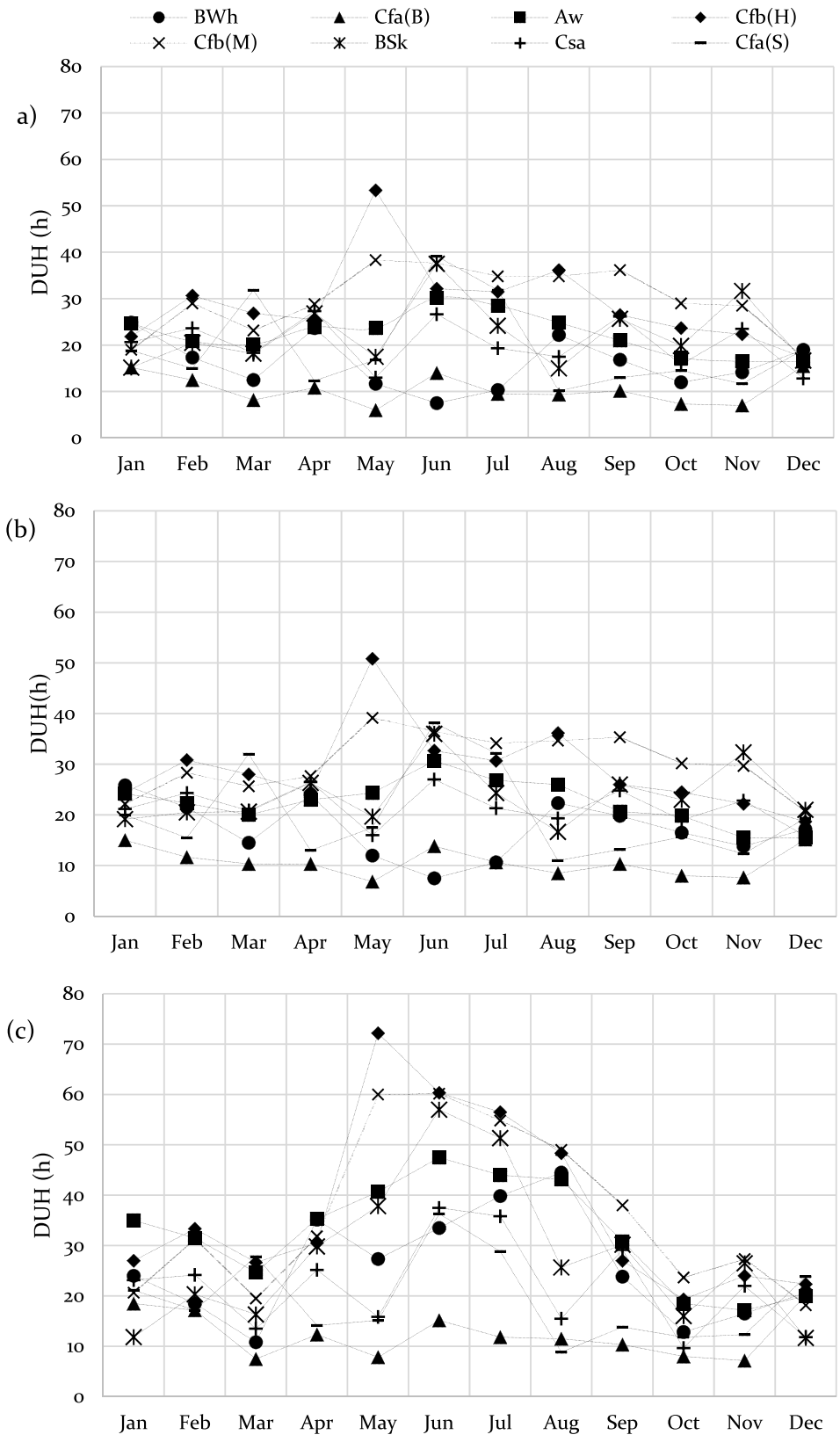

Fig. C4. Baseline monthly DUH in (a) Living room, (b) Rumpus and (c) Study room.

References

[1] Aye L., Mirza M.A. A review of sustainability assessment tools for office buildings. In: 40th Annual Conference of the Architectural Science Association ANZAScA, Adelaide, Australia. 2006:382-90.
[2] WGBC. Global Status Report. London: World Green Building Council; 2017. https://www.worldgbc.org/news-media/global-status-report-2017.
[3] IEA. Energy Consumption By Sector. Paris: International Energy Agency; 2020. https://www.eia.gov/totalenergy/data/monthly/pdf/sec2.pdf.
[4] DISER. Australian Energy Update 2020. Australian Energy Statistics. Canberra: Department of Industry, Science, Energy and Resources; 2020.
[5] Aye L, Ngo T, Crawford RH, Gammampila R, Mendis P. Life cycle greenhouse gas emissions and energy analysis of prefabricated reusable building modules. Energy Build 2012;47:159–68. https://doi.org/10.1016/j.enbuild.2011.11.049.
[6] Yoon S-H. An integrative approach: Environmental quality (EQ) evaluation in residential buildings. Michigan (US): University of Michigan; 2008 [PhD thesis]:.
[7] Chiazor M. The Effects of Energy Efficient Design and Indoor Envirnomental Quality in New Office Buildings. The University of Melbourne; 2009 [PhD thesis].
[8] Haverinen-Shaughnessy U, Shaughnessy RJ, Cole EC, Toyinbo O, Moschandreas DJ. An assessment of indoor environmental quality in schools and its association with health and performance. Build Environ 2015;93:35–40. https://doi.org/10.1016/j.buildenv.2015.03.006.
[9] Veitch J.A., Galasiu A.D. The physiological and psychological effects of windows, daylight, and view at home: review and research agenda. Research Report no. IRC-RR-325: (National Research Council of Canada. Institute for Research in Construction); 2012.
[10] Edwards L, Torcellini P. Literature review of the effects of natural light on building occupants. National Renewable Energy Lab.: Golden, CO.(US) 2002.
[11] Vagner I-I. The Rehabilitation of Collective Residential Buildings. In: Bulletin of the Polytechnic Institute of Jassy - Construction Archtecture Section; 2012. p. 175–86.
[12] Tokarik MS. A multi-objectice optimization analysis of passive energy conservation measures in toronto house. Toronto, Ontario, Canada: Ryerson University; 2015 [Master's thesis].
[13] Steinhardt DA, Manley K, Miller W. Profiling the nature and context of the Australian prefabricated housing industry. Report, Queensland, Australia: Queensland University of Technology; 2013.
[14] Szokolay SV. Solar energy and building. Technical Report NASA STI/Recon 1975.
[15] Boafo FE, Kim J-H, Kim J-T. Performance of modular prefabricated architecture: case study-based review and future pathways. Sustainability 2016;8:558. https://doi.org/10.3390/su8060558.
[16] Nicol F, Humphreys M, Roaf S. Adaptive Thermal Comfort: Principles and Practice. London: Routledge; 2012.
[17] Ozarisoy B, Elsharkawy H. Assessing overheating risk and thermal comfort in state-of-the-art prototype houses that combat exacerbated climate change in UK. Energy Build 2019;187:201–17. https://doi.org/10.1016/j.enbuild.2019.01.030.
[18] Sonnick S, Erlbeck L, Gaedtke M, Wunder F, Mayer C, Krause MJ, et al. Passive room conditioning using phase change materials—Demonstration of a long-term real size experiment. Int J Energy Res 2020. https://doi.org/10.1002/er.5406.
[19] White K., Campbell J., Cheong C. Impact of poor building design and materials in overseas and off-site constructed modular buildings–A case study of an IEQ investigation into the assembly of pre-fabricated buildings in a hot and humid climate. In: AIOH 33rd Annual Conference & Exhibition, Western Australia. 2015.
[20] Shendell DG. Assessment of organic compound exposures, thermal comfort parameters, and HVAC system-driven air exchange rates in public school portable classrooms in California. Los Angeles, CA (US): University of California; 2004 [PhD thesis].
[21] Newton C, Backhouse S, Aibinu AA, Cleveland B, Crawford RH, Holzer D, et al. Plug n Play: Future prefab for smart green schools. Buildings 2018;8:88. https://doi.org/10.3390/buildings8070088.
[22] Petrosova DV, Petrosov DV. The energy efficiency of residential buildings with light walling 2014;941:814–20.
[23] Ozarisoy B, Altan H. Low-energy design strategies for retrofitting existing residential buildings in Cyprus. Proceedings of the Institution of Civil Engineers - Engineering Sustainability 2019;172:241–55. https://doi.org/10.1680/jensu.17.00061.
[24] Yıldız Y, Arsan ZD. Identification of the building parameters that influence heating and cooling energy loads for apartment buildings in hot-humid climates. Energy 2011;36:4287–96. https://doi.org/10.1016/j.energy.2011.04.013.
[25] Chen X, Yang H, Zhang W. A comprehensive sensitivity study of major passive design parameters for the public rental housing development in Hong Kong. Energy 2015;93:1804–18. https://doi.org/10.1016/j.energy.2015.10.061.
[26] Wang Y, Kuckelkorn J, Zhao F-Y, Spliethoff H, Lang W. A state of art of review on interactions between energy performance and indoor environment quality in Passive House buildings. Renew Sust Energy Rev 2017;72:1303–19. https://doi.org/10.1016/j.rser.2016.10.039.
[27] Chen X, Yang H. Integrated energy performance optimization of a passively designed high-rise residential building in different climatic zones of China. Appl Energy 2018;215:145–58. https://doi.org/10.1016/j.apenergy.2018.01.099.
[28] Nutkiewicz A, Jain RK, Bardhan R. Energy modeling of urban informal settlement redevelopment: Exploring design parameters for optimal thermal comfort in Dharavi, Mumbai. India. Appl Energy 2018;231:433–45. https://doi.org/10.1016/j.apenergy.2018.09.002.
[29] Gagnon R, Gosselin L, Decker S. Sensitivity analysis of energy performance and thermal comfort throughout building design process. Energy Build 2018;164:278–94. https://doi.org/10.1016/j.enbuild.2017.12.066.
[30] Dave M, Watson B, Prasad D. Performance and perception in prefab housing: An exploratory industry survey on sustainability and affordability. Procedia Eng 2017;180:676–86. https://doi.org/10.1016/j.proeng.2017.04.227.
[31] Mourshed M. Climatic parameters for building energy applications: A temporal-geospatial assessment of temperature indicators. Renew Energy 2016;94:55–71. https://doi.org/10.1016/j.renene.2016.03.021.
[32] Saltelli A, Ratto M, Andres T, Campolongo F, Cariboni J, Gatelli D, et al. Global sensitivity analysis: the primer. John Wiley & Sons; 2008.
[33] Reuter U, Liebscher M. Global sensitivity analysis in view of nonlinear structural behavior. In: LSDYNA Anwenderforum. Bamberg 2008.
[34] Tian W. A review of sensitivity analysis methods in building energy analysis. Renew Sustain Energy Rev 2013;20:411–9. https://doi.org/10.1016/j.rser.2012.12.014.
[35] Tarantola S. SimLab 2.2 Reference Manual. Ispra, Italy: Institute for Systems, Informatics and Safety, European Commission. Joint Research Center 2005.
[36] Yildiz Y, Korkmaz K, Özbalta TG, Arsan ZD. An approach for developing sensitive design parameter guidelines to reduce the energy requirements of low-rise apartment buildings. Appl Energy 2012;93:337–47. https://doi.org/10.1016/j.apenergy.2011.12.048.
[37] Ignjatović MG, Blagojević BD, Stojiljković MM, Mitrović DM, Anđelković AS, Ljubenović MB. Sensitivity analysis for daily building operation from the energy and thermal comfort standpoint. Therm Sci 2016;20:1485–500. https://doi.org/10.2298/TSCI16S5485I.
[38] Li H, Wang S, Cheung H. Sensitivity analysis of design parameters and optimal design for zero/low energy buildings in subtropical regions. Appl Energy 2018;228:1280–91. https://doi.org/10.1016/j.apenergy.2018.07.023.
[39] Naji S, Aye L, Noguchi M. Dataset on thermal properties, sound reductions, TVOC emissions, and costs of envelope components for prefabricated buildings in Australia. Mendeley Data 2020. https://doi.org/10.17632/kjjrrxddbr.2.
[40] Naji S, Aye L, Noguchi M. Multi-objective optimisations of envelope components for a prefabricated house in six climate zones. Appl Energy 2021;282:116012. https://doi.org/10.1016/j.apenergy.2020.116012.
[41] Rosso F, Ciancio V, Dell'Olmo J, Salata F. Multi-objective optimization of building retrofit in the Mediterranean climate by means of genetic algorithm application. Energy Build. 2020;109945. https://doi.org/10.1016/j.enbuild.2020.109945.
[42] Naji S. Multi-objective Optimisation of a Prefabricated House in Australian Climate Zones. The University of Melbourne; 2020 [PhD Thesis].
[43] Peel MC, Finlayson BL, McMahon TA. Updated world map of the Köppen-Geiger climate classification. Hydrol Earth Syst Sci 2007;11:1633–44. https://hal.archives-ouvertes.fr/hal-00298818.
[44] ABCB. National Construction Code, Building Code of Australia: Australian Building Codes Board; 2019.
[45] Meteonorm. Meteonorm Features, http://www.meteonorm.com; 2019 [20 December 2019].
[46] Bern C, Huguenin-landl B, Studer C. Meteonorm - Global Meteorological Database, Handbook Part I: Software Global Meteorological Database Version 7 Software and Data for Engineers. Bern, Switzerland: Meteotest; 2017.
[47] U.S. Department of Energy. EnergyPlus™ Version 9.4.0 Documentation,. Weather Converter Program. National Renewable Energy Laboratory (NREL); 2020.
[48] U.S. Department of Energy. Input output reference, The Encyclopedic Reference to EnergyPlus™ Input and Output. National Renewable Energy Laboratory (NREL). 2012. p. 1996–2015.
[49] Liggett R., Milne M. Climate Consultant 6.0 (Build 13); 2020 [20 November 2020], http://www.energy-design-tools.aud.ucla.edu/climate-consultant/request-climate-consultant.php.
[50] ASHRAE. ASHRAE Handbook-Fundamentals: American society of Heating Refrigerating and Air-Conditioning Engineers; 2009.
[51] Australian Government Bureau of Meteorology. Annual and monthly heating and cooling degree days; [1 October 2019], http://www.bom.gov.au/climate/map/heating-cooling-degree-days/documentation.shtml.
[52] Habitech Systems. Project Spotlight: Hampton House; 2020 [11 November 2020], https://www.habitechsystems.com.au/news/project-spotlight-hampton-house.
[53] NatHERS. Software Accreditation Protocol. Nationwide House Energy Rating Scheme; 2012. p. 24.
[54] Solar Energy Laboratory. Multizone Building modeling with Type56 and TRNBuild. TRNSYS 18 Documentation. University of Wisconsin-Madison2017.
[55] Dussault J-M, Gosselin L. Office buildings with electrochromic windows: A sensitivity analysis of design parameters on energy performance, and thermal and visual comfort. Energy Build 2017;153:50–62. https://doi.org/10.1016/j.enbuild.2017.07.046.
[56] Reinhart C. Daysim Advanced Daylight Simulation Software; 2018, https://daysim.ning.com.
[57] Radiance. Radiance Synthetic Imaging System. 2018. [2019], http://radsite.lbl.gov/radiance.
[58] JEPlus. JEPlus – An EnergyPlus simulation manager for parametrics; 2018 [5 September 2019], http://www.jeplus.org/wiki/doku.php.
[59] SimLab. SIMLAB and other software. 2018. [2019], https://ec.europa.eu/jrc/en/samo/simlab.
[60] Sustainability Victoria. Heat your home efficiently; [26 February 2021]. https://www.sustainability.vic.gov.au/You-and-your-home/Save-energy/Heating/Heat-your-home-efficiently.
[61] Trcka M., Loonen R., Hensen J., Houben J. Computational building performance simulation for integrated design and product optimization. In: Proceedings of Building Simulation, 12th Conference of International Building Performance Simulation Association, Sydney, Australia. 2011.

[62] Chen X, Yang H, Wang Y. Parametric study of passive design strategies for high-rise residential buildings in hot and humid climates: miscellaneous impact factors. Renew Sust Energy Rev 2017;69:442–60. https://doi.org/10.1016/j.rser.2016.11.055.
[63] Thermal Environmental Conditions for Human Occupancy: ANSI/ASHRAE Standard 55-2017 (Supersedes ANSI/ASHRAE Standard 55-2013) Includes ANSI/ASHRAE Addenda Listed in Appendix N. ASHRAE, 2017.
[64] Asadi E, da Silva MG, Antunes CH, Dias L, Glicksman L. Multi-objective optimization for building retrofit: A model using genetic algorithm and artificial neural network and an application. Energy Build 2014;81:444–56. https://doi.org/10.1016/j.enbuild.2014.06.009.
[65] Interior and workplace lighting. Part 1 : General principles and recommendations (AS/NZS 1680.1:2006). Australia/New Zealand: Standards Australia, 2006.
[66] Rokach L, Maimon O. Clustering methods. Data mining and knowledge discovery handbook. Springer; 2005. p. 321–52.
[67] IBM. IBM SPSS Statistics for Windows. [28 January 2020]. https://www.ibm.com/au-en/products/spss-statistics?lnk=STW_AU_MAST_P4_TL&lnk2=learn_SPSSstatSub.
[68] Hair JF, Black WC, Babin BJ, Anderson RE. Multivariate data analysis: Pearson new international edition. Essex: Pearson Education Limited; 2014. p. 415–31.
[69] Building Air Tightness Innovation Challenges Handbook. Australia, Green Building Council of Australia; 2015.
[70] Zhangjiagang Leader. MGO Board; 2016 [5 September 2019], https://www.zjgleader.com/projects/mgo-wall-partition.
[71] Australian Urethane & Styrene. Expanded polystyrene (EPS) technical data; [5 September 2019], https://www.thermalps.com.au/imagesDB/wysiwyg/TDS_Expanded_Polystyrene.pdf.
[72] CSR GYPROCK. Supaceil; 2019 [5 September 2019]. https://www.gyprock.com.au/products/plasterboard-supaceil.
[73] TRAINENERGY. Resistance of air layers and surface layers, ; 2009 [5 September 2019].
[74] Rambaldi E, Prete F, Bignozzi MC. Acoustic and thermal performances of ceramic tiles and tiling systems. Ceram Int 2015;41:7252–60. https://doi.org/10.1016/j.ceramint.2015.03.032.
[75] Solar Energy Laboratory. Standard Component Library Overview. TRNSYS 18 Documentation. University of Wisconsin-Madison; 2017.
[76] Ambrose M, Syme M. Air tightness of new Australian residential buildings. Procedia Eng 2017;180:33–40.
[77] Naji S, Aye L, Noguchi M. Dataset on validation of TRNSYS building model for a prefabricated house built in Australia. Mendeley Data 2020;1. https://doi.org/10.17632/79c96pz77j.1.
[78] Naji S, Aye L, Noguchi M. Dataset on baseline performance and sensitivity analysis of a prefabricated house in six climate zones in Australia. Mendeley Data 2020;1. https://doi.org/10.17632/zyy8sd479t.1.